Electronic Supplementary Information for:

Ratiometric near-infrared fluorescent probe for nitroreductase activity enables 3D imaging of hypoxic cells within intact tumor spheroids

Janeala J. Morsby,[a] Zhumin Zhang,[a] Alice Burchett,[b] Meenal Datta,[b]* and Bradley D. Smith[a]*

a. Department of Chemistry and Biochemistry
251 Nieuwland Science Hall,
University of Notre Dame
Notre Dame, IN, 46556, USA
*E-mail: smith.115@nd.edu

b. Department of Aerospace and Mechanical Engineering
145 Multidisciplinary Engineering Research Building,
University of Notre Dame
Notre Dame, IN, 46556, USA
*E-mail: mdatta@nd.edu

1. General Materials and Methods

Organic reactions were performed under an atmosphere of argon using anhydrous solvents unless otherwise noted. Reagents and solvents were purchased from Sigma-Aldrich, VWR, Oakwood, Alfa Aesar, and Thermo Fisher and used without further purification. Column Chromatography was performed using Biotage Sfär C18 Duo columns (part # FSUD-0401). Reverse phase thin layer chromatography (TLC) experiments were performed on C18 TLC plates with F254s indicator (MilliporeSigma, part # 1.15683). ^{1}H NMR spectra were recorded on Bruker 400, 500, and 800 MHz spectrometers. Multiplicities were given as singlet (s), broad signal (br), doublet (d), doublet of doublets (dd), triplet (t), or multiplet (m). Chemical shifts are presented in ppm and referenced by residual solvent peaks. High-resolution mass spectrometry (HRMS) was performed using a time-of-flight (TOF) analyzer with electrospray ionization (ESI). Absorption spectra were recorded on an Evolution 201 UV/vis spectrometer with Thermo Insight software. Fluorescence spectra were collected on a Horiba Fluoromax-4 fluorometer with FluoroEssence software. Analyte solutions were prepared in HPLC grade water (Sigma-Aldrich), HPLC grade dimethyl sulfoxide (Sigma-Aldrich), or phosphate buffered saline (Thermo Fisher). All absorption and fluorescence spectra were collected using quartz cuvettes (1 mL, 1 cm path length; for emission and excitation spectra, slit width = 2 nm, unless stated otherwise).

2. Synthesis

In short, **RNP** and **RNP$_{on}$** were prepared by conducting copper-catalyzed azide-alkyne cycloaddition reactions that attached azido Cy5 dye **1** to one of the two alkyne groups within symmetrical Cy7 dyes **2** or **3**, and added a hydrophilic azido carboxylate to the other alkyne group. **Note: atom assignments on ^{1}H NMR spectra, provided for reader convenience, are based on precedence from unambiguous spectra of cyanine dye homologues,[2] but they have not been confirmed by correlation NMR experiments.**

2.1 Synthesis of Cy5 dye 1.

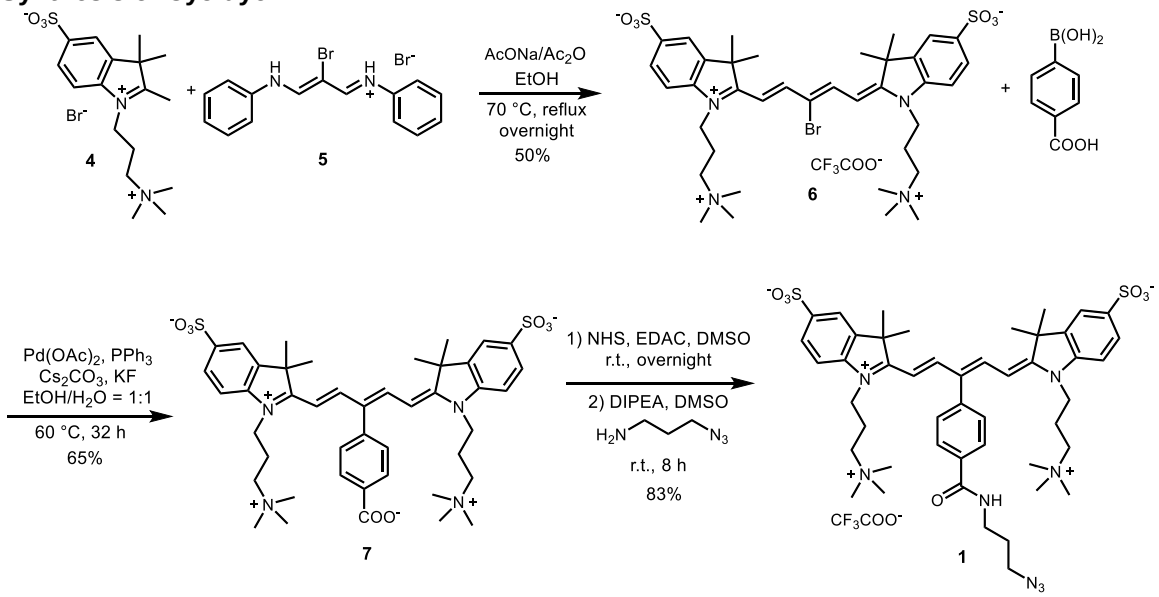

Scheme S1. Synthesis of azido Cy5 dye **1**.

2.1.1 Synthesis of Cy5 dye 6. The known compound was synthesized following a literature procedure.[1] A mixture of **4** (1.375 g, 3.30 mmol, 2.5 equiv.), *N*-((1*E*,2*Z*)-2-bromo-3-(phenylamino)allylidene)benzenaminium bromide **5** (0.5 g, 1.30 mmol, 1.0 equiv.), sodium acetate (0.53 g, 3.9 mmol, 3.0 equiv.), and acetic anhydride (5 mL) in EtOH (10 mL) was stirred at 70 °C overnight under argon in the dark. The solvent was evaporated from the reaction mixture under reduced pressure. The residue was purified by reverse phase column chromatography (C18, 0-30%, methanol containing 0.5% TFA in H_2O). The product was obtained as a blue solid (504.7 mg, 50%). ^{1}H NMR (400 MHz, DMSO-d_6) δ (ppm): 8.59 (d, J = 12.7 Hz, 2H), 7.93 (s, 2H), 7.70 (d, J = 8.7 Hz, 2H), 7.48 (d, J = 8.4 Hz, 2H), 6.34 (d, J = 13.6 Hz, 2H), 4.31-4.16 (m, 4H), 3.53-3.44 (m, 4H), 3.07 (s, 18 H), 2.25-2.12 (m, 4H), 1.76 (s, 12H).

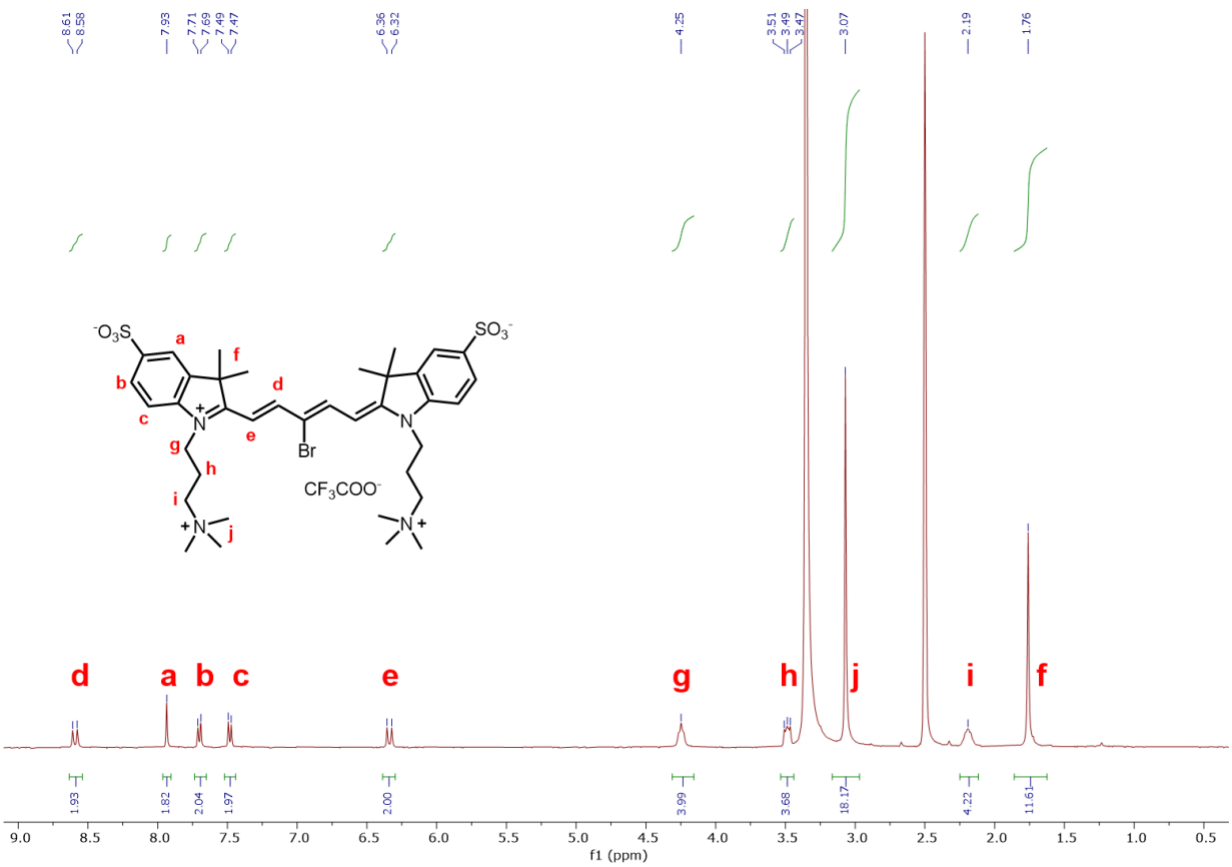

^{1}H NMR spectrum (400 MHz, DMSO-d_6, 25°C) of **6**

2.1.2 Synthesis of Cy5 dye 7. To a solution of compound **6** (0.1 g, 0.115 mmol), 4-carboxyphenylboronic acid (0.045 g, 0.232 mmol), potassium fluoride (15.9 mg, 0.273 mmol), and cesium carbonate (88.9 mg, 0.273 mmol) in a mixture of EtOH (4 mL) and water (4 mL) under argon at room temperature, was added palladium acetate (2.25 mg, 0.01 mmol) and triphenylphosphine (12.1 mg, 0.04 mmol). The reaction mixture was stirred at 60 °C for 16 h in the dark. A second batch of boronic acid (6.8 mg, 0.035 mmol), palladium acetate (2.25 mg, 0.01 mmol) and triphenylphosphine (12.1 mg, 0.04 mmol) was added to the reaction mixture under argon and it was stirred at 60 °C for another 16 h in the dark. The reaction progress was monitored by TLC. The solvent was evaporated from the reaction mixture under vacuum. The residue was purified by reverse phase column chromatography (C18, 0-40%, methanol containing 0.5% TFA in H_2O). The product was obtained as a blue solid (62.4 mg, 65%). ^{1}H NMR (400 MHz, DMSO-d_6) δ (ppm): 8.55 (d, J = 13.7 Hz, 2H), 7.98 (d, J = 9.6 Hz, 2H), 7.87 (s, 2H), 7.64 (d, J = 8.2 Hz, 2H), 7.36 (d, J = 8.4 Hz, 2H), 7.21 (d, J = 7.7 Hz, 2H), 5.60 (d, J = 14.3 Hz, 2H), 3.84-3.72 (m, 4H), 3.13-3.05 (m, 4H), 2.99 (s, 18 H), 1.94-1.84 (m, 4H), 1.78 (s, 12H).

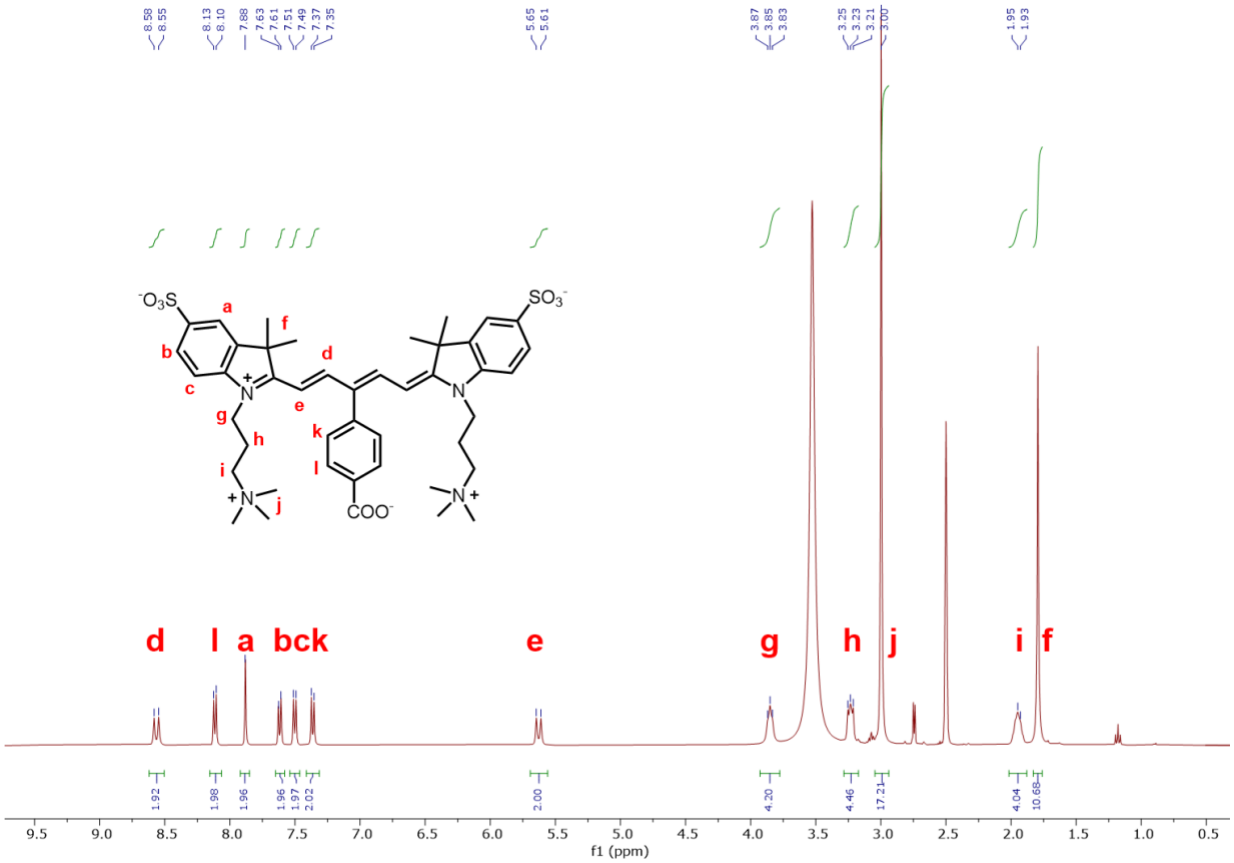

^{1}H NMR spectrum (400 MHz, DMSO-d_6, 25°C) of **7**

2.1.3 Synthesis of Cy5 dye 1. A mixture of the compound **7** (42.4 mg, 0.051 mmol), *N*-hydroxysuccinimide (17.5 mg, 0.153 mmol) and *N*-(3-dimethylaminopropyl)-*N*'-ethylcarbodiimide hydrochloride (29.2 mg, 0.153 mmol) in DMSO (4.2 mL, 0.1 mL for 1 mg of compound **7**) was stirred at room temperature in the dark. The reaction was transferred into a centrifuge tube. Ethyl acetate (5 mL for 1 mL of DMSO) was added to the tube and mixture was centrifuged at 3600 rpm for 5 min. The supernatant was discarded and the solid was washed with ethyl acetate (2x) and diethyl ether (1x) then dried in vacuo to afford the NHS-ester intermediate with quantitative yield. It was used for next step without purification. Then a mixture of NHS-ester intermediate, 3-azidopropylamine (12.7 mg, 0.127 μmol) and diisopropyl ethyl amine (44.9 μL, 0.254 mmol) in DMSO (4 mL) was stirred at room temperature in the dark for 8 h. The mixture was directly purified by reverse phase column chromatography (C18, 0-40% MeOH containing 0.5% TFA in H_2O) to afford the product as a blue solid (43 mg, 83%). ^{1}H NMR (400 MHz, DMSO-d_6) δ (ppm): 8.57 (d, J = 15.4 Hz, 2H), 8.05 (d, J = 8.1 Hz, 2H), 7.90 (d, J = 1.7 Hz, 2H), 7.65 (d, J = 8.2 Hz, 2H), 7.47 (d, J = 7.8 Hz, 2H), 7.36 (d, J = 8.8 Hz, 2H), 5.63 (d, J = 13.1 Hz, 2H), 3.89-3.79 (m, 4H), 3.66-3.57 (m, 10H), 2.98 (s, 18 H), 1.99-1.89 (m, 4H), 1.80 (s, 12H). HRMS (ESI-TOF) m/z calcd $C_{47}H_{63}N_8O_7S_2^+$ $[M]^+$ 915.4256, found 915.4241.

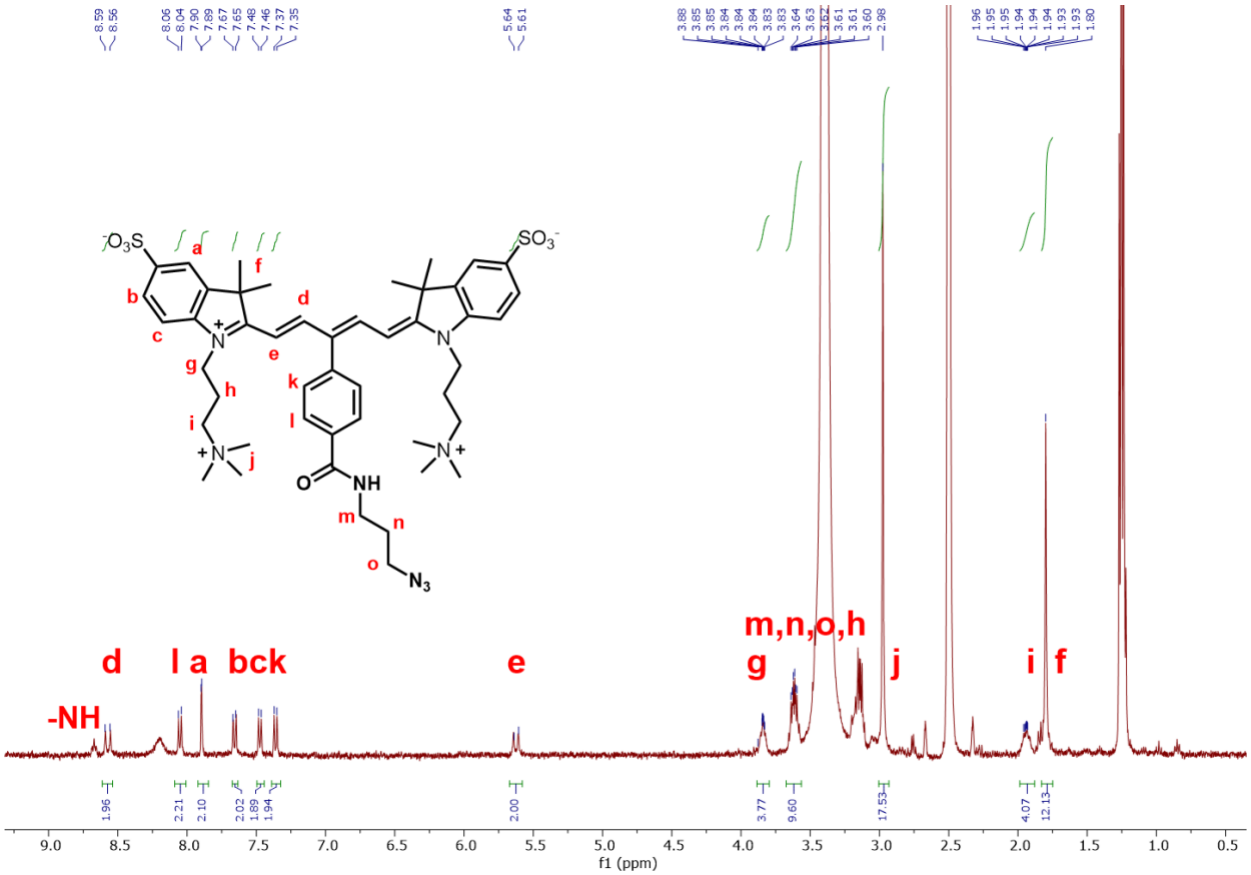

^{1}H NMR spectrum (400 MHz, DMSO-d_6, 25°C) of **1**

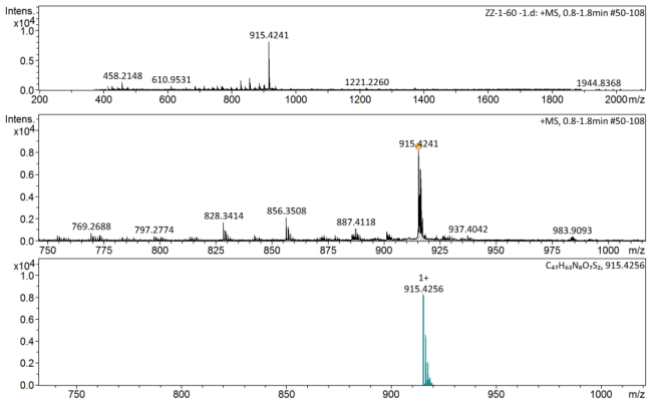

HRMS (ESI-TOF) spectrum of Cy5 dye **1**

2.2 Syntheses of Cy7 dyes 2 and 3.

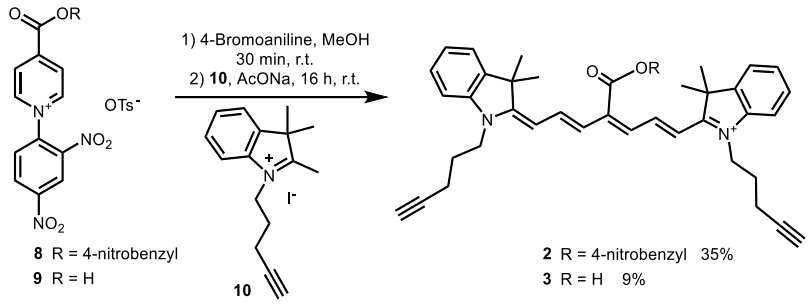

Scheme S2. Syntheses of Cy7 dyes **2** and **3**.

Intermediate compounds **8** and **9** were prepared by methods previously reported by our group.[2] Intermediate compound **10** was synthesized according to a literature procedure.[3]

General procedure for syntheses of Cy7 dyes 2 and 3. A mixture of compound **8** or **9** (0.225 mmol, 1 equiv.) and 4-bromoaniline (0.270 mmol, 1.2 equiv.) in methanol (2 mL) was stirred for 30 min at room temperature, followed by the addition of compound **10** (0.675 mmol, 3.0 equiv.) and sodium acetate (1.350 mmol, 6.0 equiv.) at the same time. The reaction was stirred overnight at room temperature in the dark. Then diethyl ether (10 mL) was added to the mixture and the flask was stored in a -20 °C freezer for 30 min. The precipitate was collected by vacuum filtration and then purified by column chromatography (SiO_2, 0-10% MeOH in DCM) to afford the product **2** (63.3 mg, 35%) or **3** (10.6 mg, 9%) as a green solid.

Compound **2**: ^{1}H NMR (400 MHz, DMSO-d_6) δ 8.32 (d, J = 8.8 Hz, 2H), 7.88-7.73 (m, 4H), 7.56 (d, J = 7.5 Hz, 2H), 7.43 (d, J = 6.5 Hz, 2H), 7.27 (d, J = 6.6 Hz, 2H), 6.67 (d, J = 13.2 Hz, 2H), 6.56 (d, J = 13.4 Hz, 2H), 5.64 (s, 2H), 4.22-4.10 (m, 4H), 2.95 (d, J = 2.6 Hz, 2H), 2.38-2.28 (m, 4H), 1.96-1.84 (m, 4H), 1.47 (s, 12H). HRMS (ESI-TOF) m/z calcd $C_{45}H_{46}N_3O_4$ $[M]^+$ 692.3483, found 692.3480.

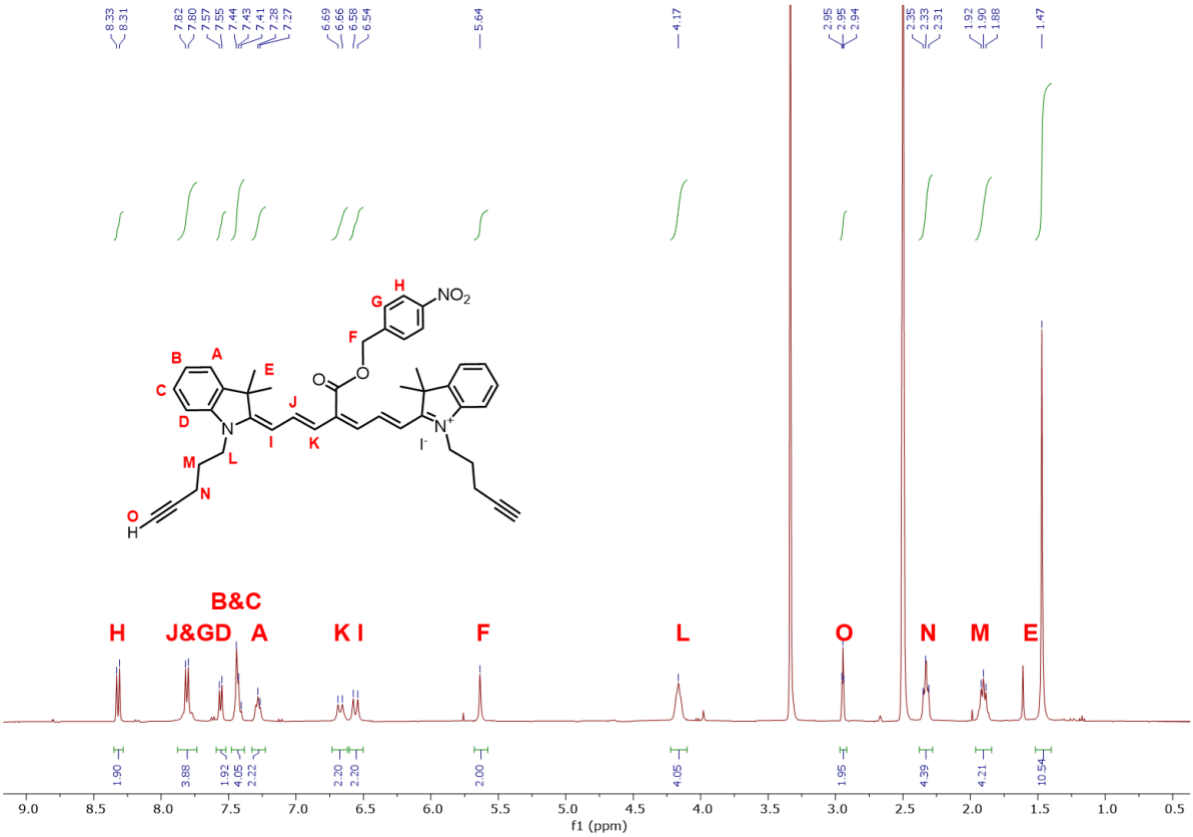

^{1}H NMR spectrum (400 MHz, DMSO-d_6, 25°C) of **2**

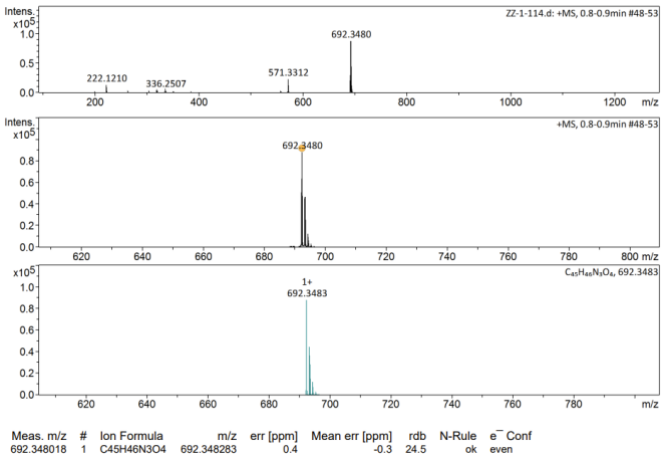

HRMS (ESI-TOF) spectrum of Cy7 dye **2**

Compound **3**: ^{1}H NMR (400 MHz, MeOD-d_4) δ 8.13 (t, J = 13.3 Hz, 2H), 7.49 (d, J = 7.4 Hz, 2H), 7.41 (d, J = 7.7 Hz, 2H), 7.31 (d, J = 8.0 Hz, 2H), 7.25 (t, J = 7.4 Hz, 2H), 6.35 (dd, J = 13.3, 5.9 Hz, 4H), 4.21 (t, J = 7.4 Hz, 4H), 2.51 (t, J = 2.6 Hz, 2H), 2.43-2.36 (m, 4H), 2.07-1.99 (m, 4H), 1.69 (s, 12H). HRMS (ESI-TOF) m/z calcd $C_{38}H_{41}N_2O_2$ $[M]^+$ 557.3163, found 557.3173.

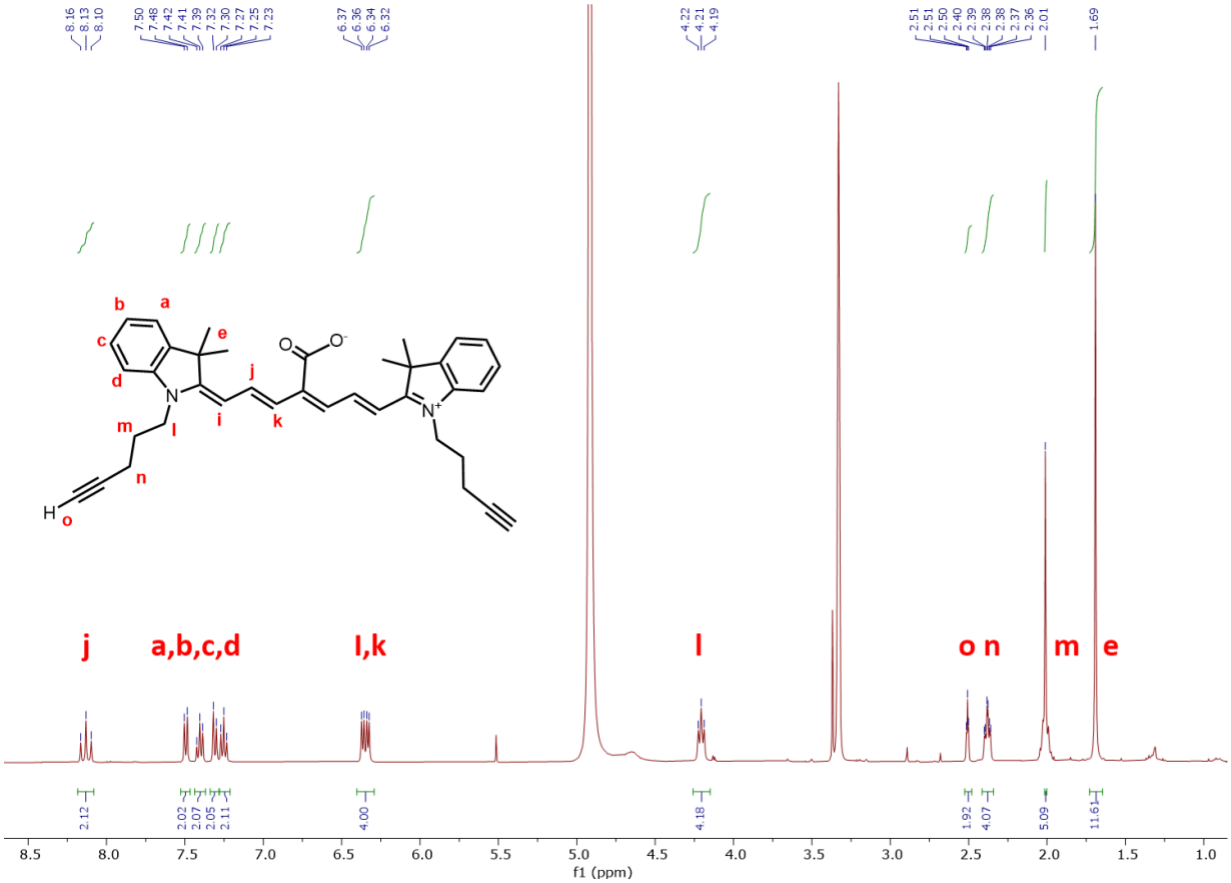

^{1}H NMR spectrum (400 MHz, MeOD-d_4, 25°C) of **3**

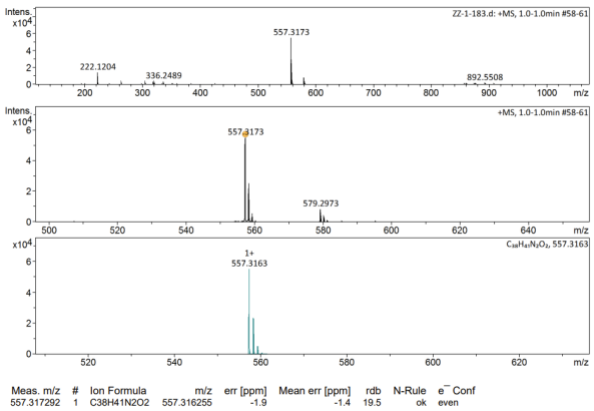

HRMS (ESI-TOF) spectrum of Cy7 dye **3**

2.3 Synthesis of ratiometric nitroreductase probe (RNP).

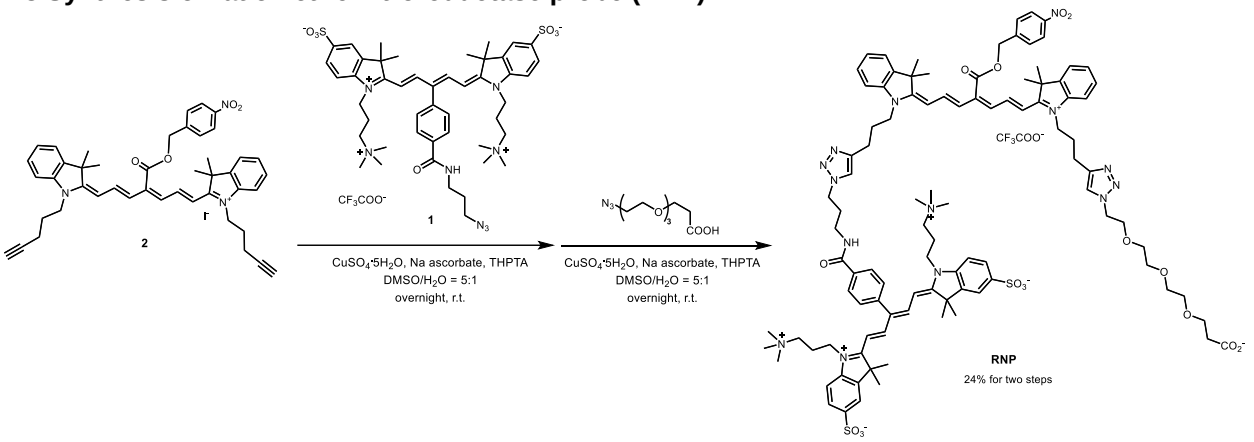

Scheme S3. Synthesis of ratiometric nitroreductase probe **(RNP)**.

To a solution of Cy7 dye **2** (31.8 mg, 0.0459 mmol, 1.0 equiv.) and Cy5 dye **1** (60.0 mg, 0.0655 mmol, 1.4 equiv.) dissolved in DMSO (2 mL), a solution of $CuSO_4{\cdot}5H_2O$ (5.8 mg, 0.0230 mmol, 0.5 equiv.), sodium ascorbate (9.1 mg, 0.0459 mmol, 1.0 equiv.), THPTA (10 mg, 0.0230 mmol, 0.5 equiv.) dissolved in H_2O (0.4 mL) was added. The reaction solution was kept stirring in the dark at room temperature overnight. Then 3-[2-[2-(2-azidoethoxy)ethoxy]ethoxy]propanoic acid (17 mg, 0.0689 mmol, 1.5 equiv.), $CuSO_4{\cdot}5H_2O$ (5.8 mg, 0.0230 mmol, 0.5 equiv.), sodium ascorbate (9.1 mg, 0.0459 mmol, 1.0 equiv.), and THPTA (10 mg, 0.0230 mmol, 0.5 equiv.) were added to the reaction mixture. The reaction solution was kept stirring in the dark at room temperature overnight. The mixture was purified by reverse phase column chromatography (C18, 40-90% MeOH containing 0.5% TFA in water) to afford the product ratiometric nitroreductase probe (**RNP**) as a blue solid (21.5 mg, 24% for two steps). ^{1}H NMR (800 MHz, DMSO-d_6) δ 8.75 (brs, 1H), 8.56 (d, J = 14.1 Hz, 2H), 8.31 (d, J = 8.7 Hz, 2H), 8.04 (d, J = 8.2 Hz, 2H), 7.98 (s, 1H), 7.92-7.88 (m, 3H), 7.87 (s, 1H), 7.82-7.79 (m, 3H), 7.65 (d, J = 8.2 Hz, 2H), 7.58-7.54 (m, 2H), 7.48-7.44 (m, 3H), 7.43-7.38 (m, 3H), 7.35 (d, J = 8.4 Hz, 2H), 7.31-7.25 (m, 2H), 6.73-6.63 (m, 2H), 6.63-6.56 (m, 2H), 5.67-5.57 (m, 4H), 4.44-4.37 (m, 4H), 4.26-4.17 (m, 4H), 3.89-3.80 (m, 4H), 3.80-3.75 (m, 2H), 3.57-3.53 (m, 2H), 3.52-3.47 (m, 2H), 3.47-3.43 (m, 4H), 3.37-3.31 (m, 4H), 3.20 (t, J = 8.3 Hz, 4H), 2.97 (s, 18H), 2.80-2.74 (m, 4H), 2.10-2.03 (m, 4H), 1.98-1,90 (m, 4H), 1.79 (s, 12H), 1.53-1.50 (m, 4H), 1.48 (s, 12H). HRMS (ESI-TOF) m/z calcd $C_{101}H_{125}N_{14}O_{16}S_2$ $[M]^+$ 1853.8834, found 1853.8812.

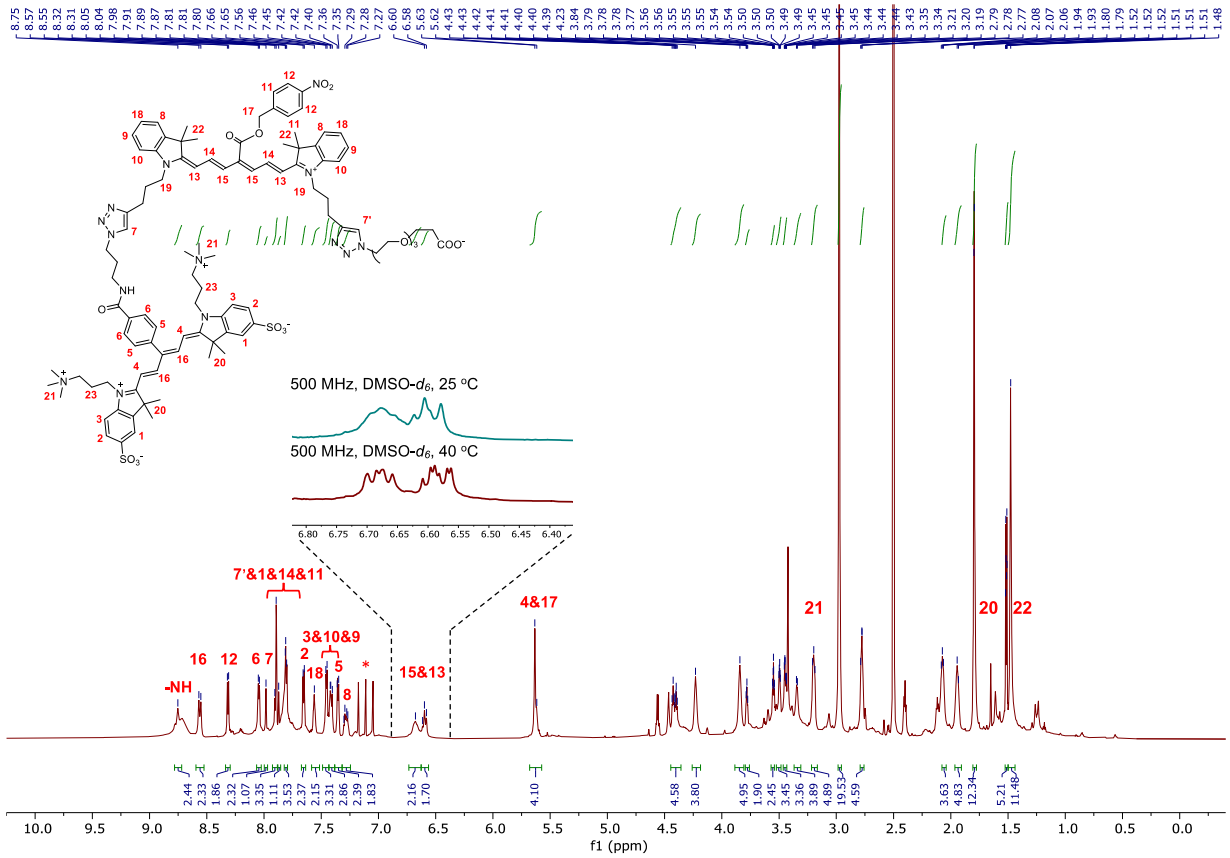

^{1}H NMR spectrum (800 MHz, DMSO-d_6, 25˚C) of **RNP**, with inserted 500 MHz spectra comparing two heptamethine peaks at two temperatures (25 and 40 ˚C). *NH_4^+ counter cation acquired during purification.

The NMR peaks for the heptamethine protons in **RNP** are relatively broad at room temperature, indicating a flexible molecular structure. Upon warming, these peaks sharpen and exhibit fine structure as seen in the inserted spectra comparing two heptamethine peaks at two temperatures. This spectral feature is consistent with the known dynamic NMR behavior of heptamethine cyanine structures.[4] In addition to the all-trans heptamethine conformation that is shown above, a small fraction of the heptamethine molecules adopt a conformation with a cis configuration about the C_{14}-C_{15} bond. Other heptamethine conformational isomers are also possible since the rotational barriers are relatively low, and the conformation exchange produces line broadening at room temperature.

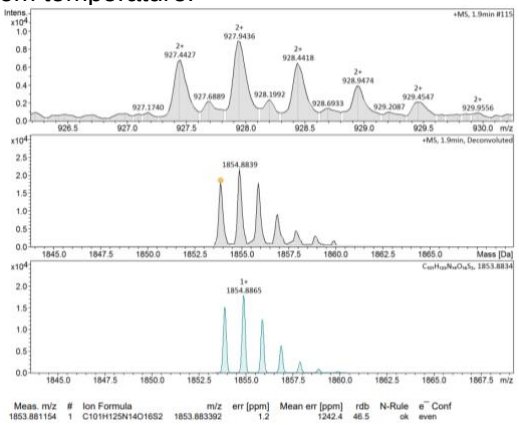

HRMS (ESI-TOF) spectrum of **RNP**

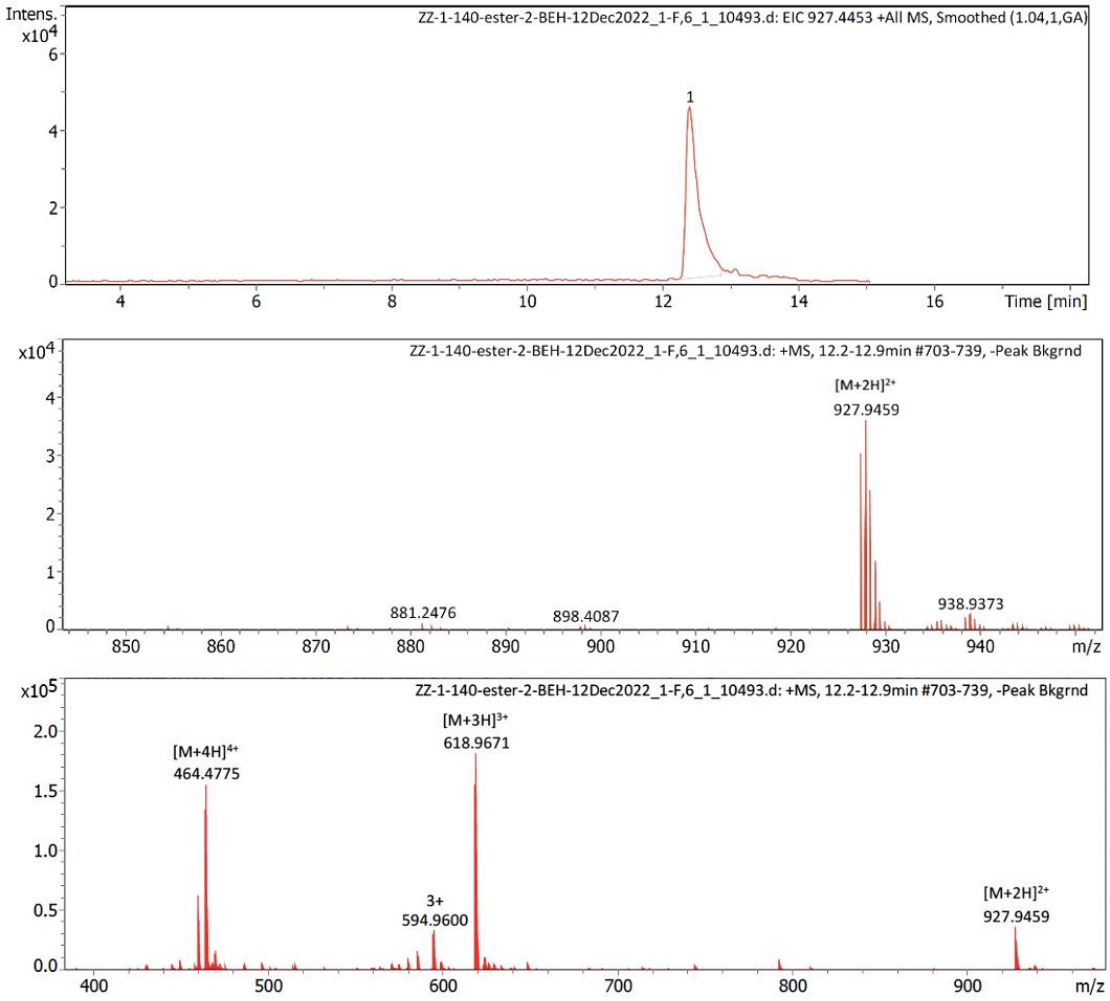

LC-MS of **RNP** indicating purity > 95% (linear gradient 0-75% acetonitrile in water with 1 mM ammonium bicarbonate), (*top*) UV chromatogram, (*middle*) scale-expanded partial MS spectrum for chromatogram peak 12.2-12.9 min, m/z = 927.9459 corresponds to $[M+H]^{2+}$. (*bottom*) complete MS spectrum of all ions detected for chromatogram peak 12.2-12.9 min, all the ions correspond to **RNP**.

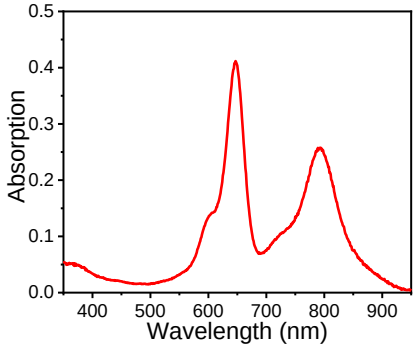

Absorption spectrum of **RNP** (4 μM) in MeOH

2.4 Synthesis of authentic RNP_{on} the "on" version of RNP.

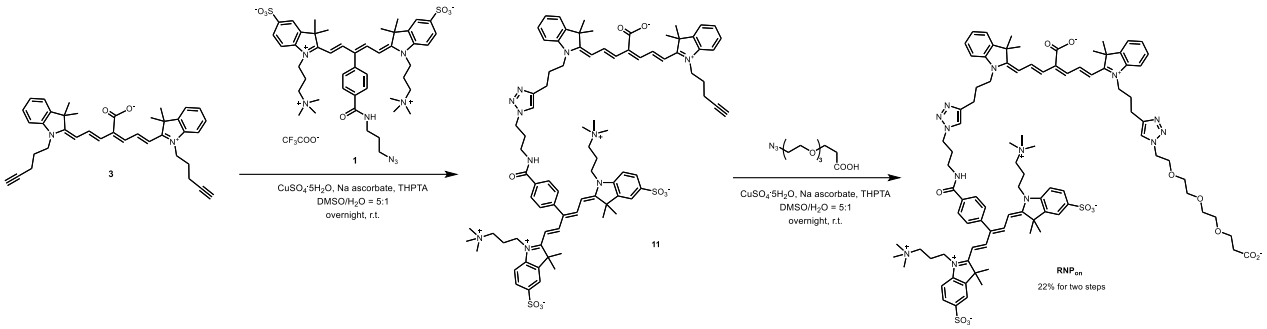

Scheme S4. Synthesis of **RNP_{on}**.

To a solution of Cy7 dye **3** (27.8 mg, 0.0499 mmol, 1.0 equiv.) and Cy5 dye **1** (31.1 mg, 0.0339 mmol, 0.68 equiv.) dissolved in DMSO (2 mL), a solution of $CuSO_4{\cdot}5H_2O$ (6.2 mg, 0.0250 mmol, 0.5 equiv.), sodium ascorbate (9.8 mg, 0.0499 mmol, 1.0 equiv.), THPTA (13.3 mg, 0.0250 mmol, 0.5 equiv.) dissolved in H_2O (0.4 mL) was added. The reaction solution was kept stirring in the dark at room temperature overnight. The mixture was purified by reverse phase column chromatography (C18, 40-90% MeOH containing 0.5% TFA in water) to afford the intermediate **11** as a blue solid (15.4 mg, 32%). To a solution of **11** and 3-[2-[2-(2-azidoethoxy)ethoxy]ethoxy] propanoic acid (14.8 mg, 0.0599 mmol, 1.2 equiv.) dissolved in DMSO (2 mL), a solution of $CuSO_4{\cdot}5H_2O$ (6.2 mg, 0.0250 mmol, 0.5 equiv.), sodium ascorbate (9.8 mg, 0.0499 mmol, 1.0 equiv.), and THPTA (13.3 mg, 0.0250 mmol, 0.5 equiv.) dissolved in H_2O (0.4 mL) was added. The reaction solution was kept stirring in the dark at room temperature overnight. The mixture was purified by reverse phase column chromatography (C18, 40-100% MeOH containing 0.5% TFA in water) to afford the product **RNP_{on}** as a blue solid (3.7 mg, 22% for two steps). ^{1}H NMR (400 MHz, DMSO-d_6) δ 8.74 (m, 1H), 8.56 (d, J = 14.1 Hz, 2H), 8.04 (d, J = 7.9 Hz, 2H), 7.99 (s, 1H), 7.93-7.86 (m, 5H), 7.68-7.59 (m, 4H), 7.48-7.38 (m, 6H), 7.35 (d, J = 8.4 Hz, 2H), 7.30-7.22 (m, 2H), 6.55 (d, J = 13.3 Hz, 2H), 5.62 (d, J = 13.9 Hz, 2H), 4.50-4.39 (m, 12 H), 4.26-4.19 (m, 4H), 3.88-3.81 (m, 4H), 3.78 (t, J = 5.3 Hz, 2H), 3.58-3.51 (m, 4H), 3.51-3.47 (m, 2H), 3.47-3.44 (m, 4H), 3.24-3.16 (m, 4H), 2.97 (s, 18H), 2.81-2.73 (m, 4H), 2.16-2.05 (m, 4H), 2.00-1.88 (m, 4H), 1.79 (s, 12 H), 1.60 (d, J = 3.3 Hz, 12H). HRMS (ESI-TOF) m/z calcd $C_{94}H_{120}N_{13}O_{14}S_2$ $[M]^+$ 1718.8514, found 1718.8498.

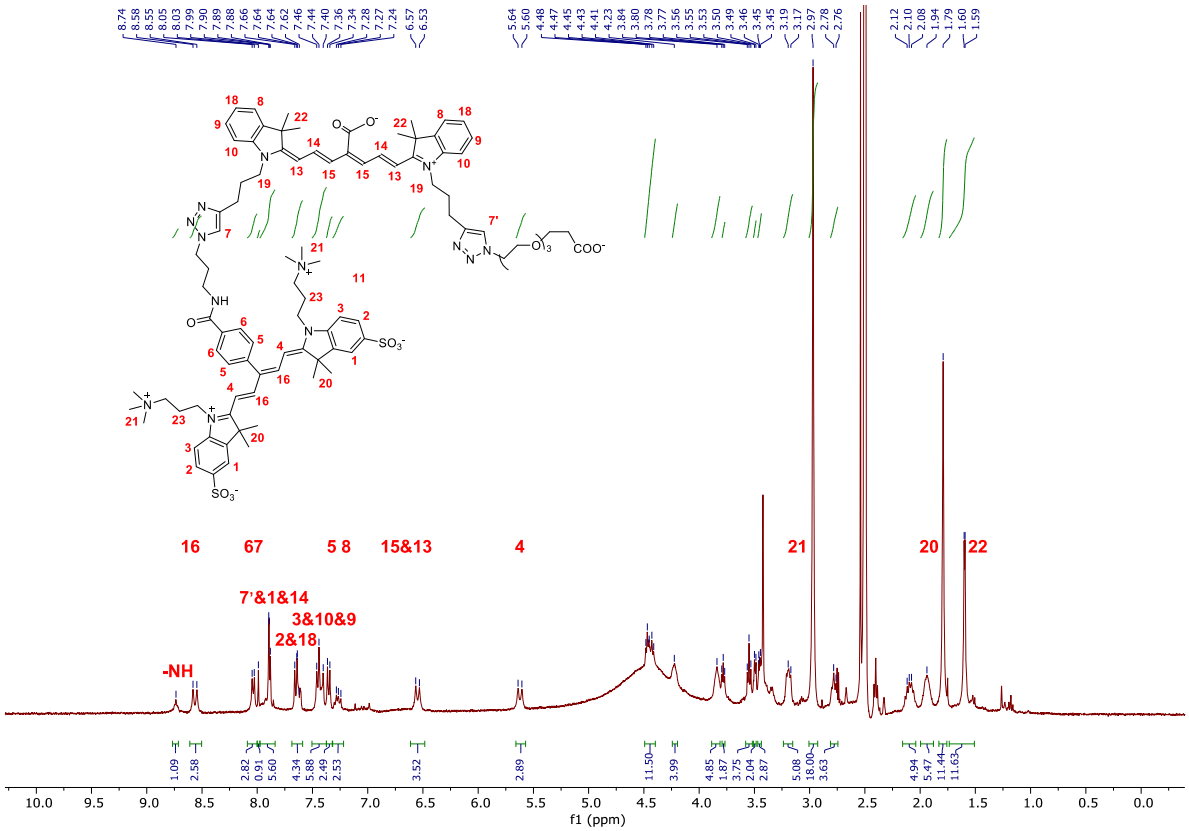

^{1}H NMR spectrum (400 MHz, DMSO-d_6, 25°C) of **RNP$_{on}$**. The broad peak at 4.5 ppm is due to adventitious water in the sample which is quite hygroscopic.

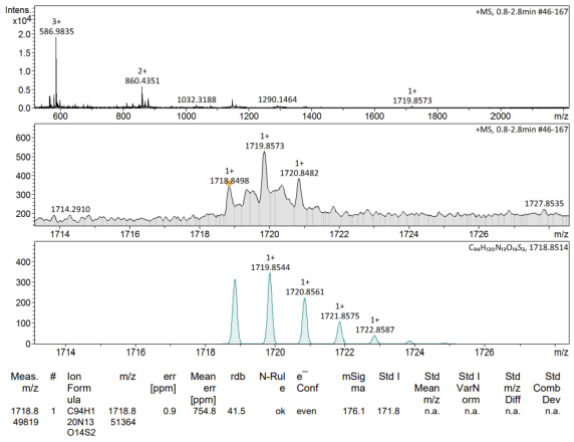

HRMS (ESI-TOF) spectrum of **RNP$_{on}$**

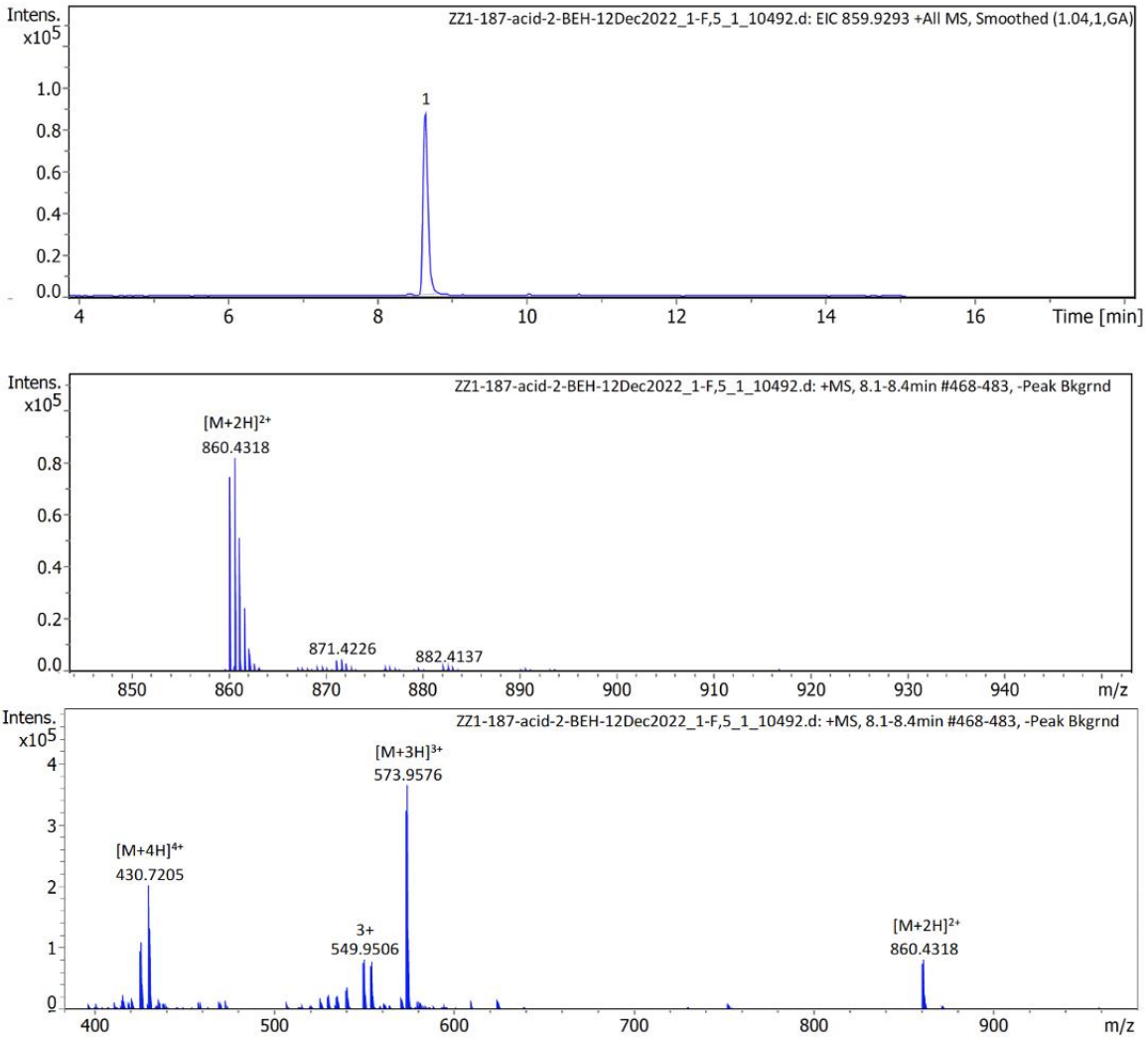

LC-MS of **RNP$_{on}$** indicating purity > 95% (linear gradient 0-75% acetonitrile in water with 1 mM ammonium bicarbonate), (*top*) UV chromatogram, (*middle*) scale-expanded partial MS spectrum for chromatogram peak 8.1-8.4 min, m/z = 860.4318 corresponds to $[M+H]^{2+}$. (*bottom*) complete MS spectrum of all ions detected for chromatogram peak 8.1-8.4 min, all the ions correspond to **RNP$_{on}$**.

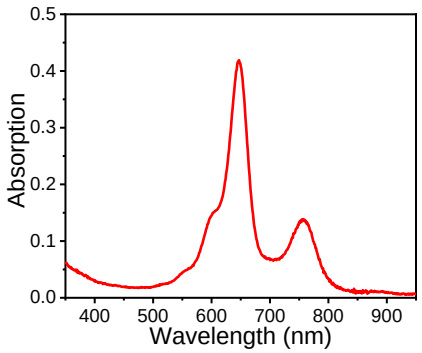

Absorption spectrum of **RNP$_{on}$** (4 µM) in MeOH

3. Computed Molecular Models of RNP and RNP_{on}.

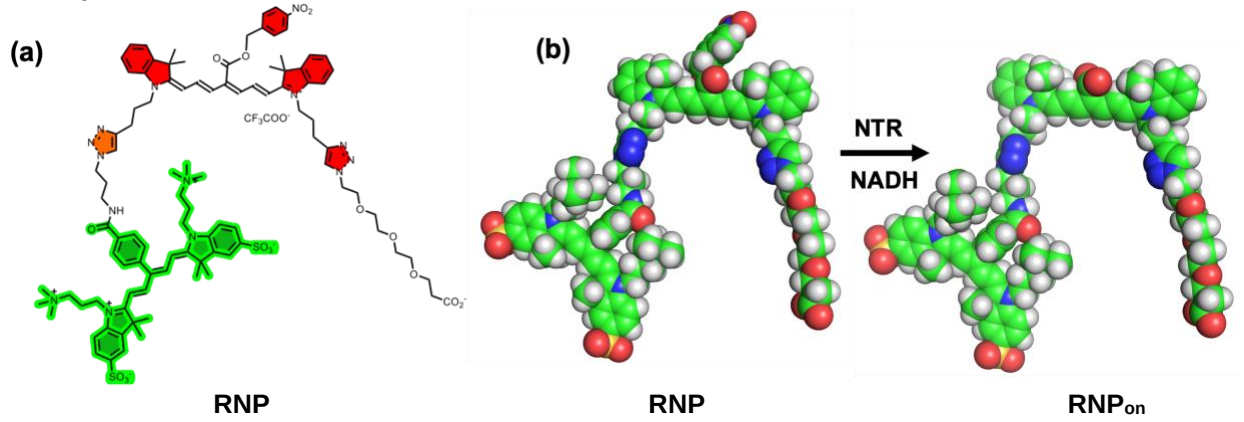

Figure S1. (a) Chemical structure of **RNP** (b) Computed models of **RNP** and **RNP_{on}** in low-energy conformations, calculated at B3LYP/6-311G(d,p) level.

4. Absorbance and Fluorescence Spectra of RNP and RNP_{on}

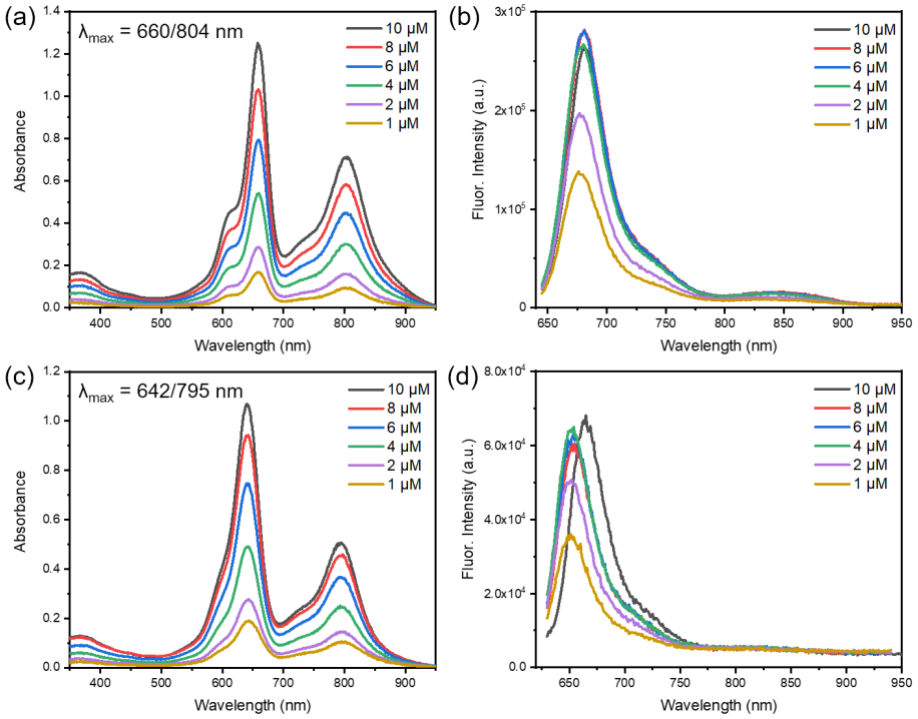

Figure S2. Absorbance and emission spectra of **RNP** at various concentrations in (a-b) DMSO (λ_{ex} = 640 nm) and in (c-d) H_2O (λ_{ex} = 620 nm) at room temperature. Slit width: 2 nm.

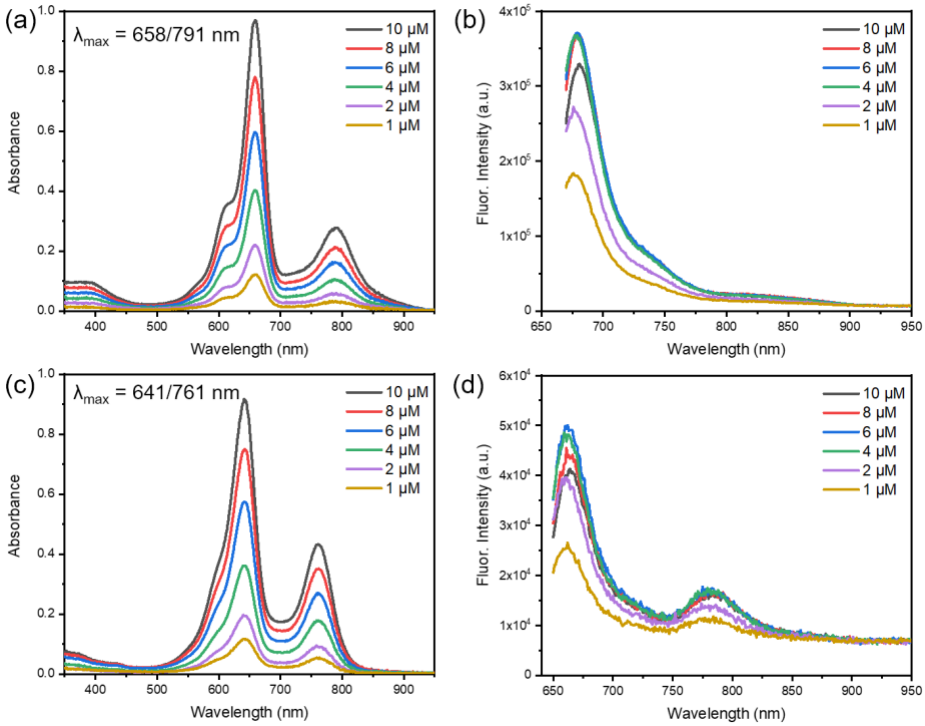

Figure S3. Absorbance and emission spectra of **RNP_{on}** at various concentrations in (a-b) DMSO (λ_{ex} = 640 nm) and in (c-d) H_2O (λ_{ex} = 640 nm) at room temperature. Slit width: 2 nm.

5. Demonstration That RNP and RNP_{on} Both Exhibit FRET

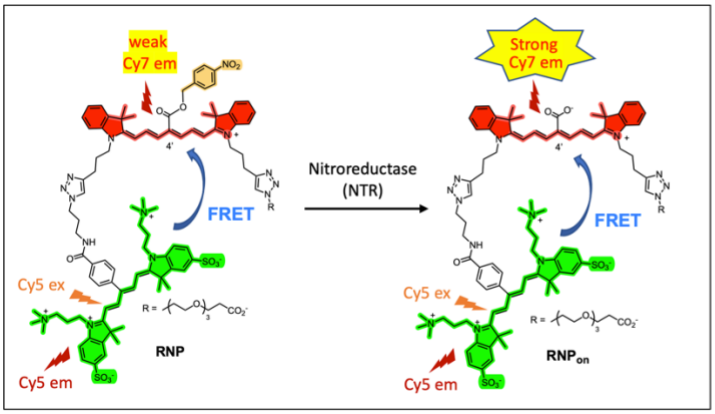

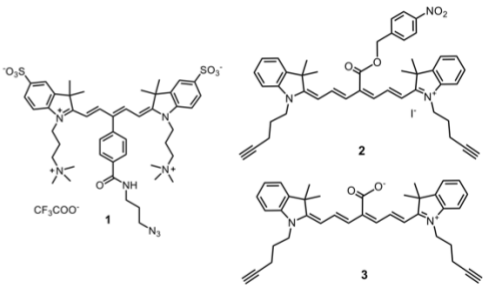

Scheme S5. (left box) Both **RNP** and **RNP_{on}** exhibit FRET from the Cy5 component (colored green) to the Cy7 component (colored red), but the Cy7 component within **RNP_{on}** emits increased fluorescence which produces a higher Cy7/Cy5 fluorescence ratio. (right) Structures of the Cy5 and Cy7 building blocks used in these FRET measurements.

The fluorescence spectra in Figure S4b,d show that the Cy5 component within **RNP** and **RNP_{on}** acts as a FRET donor, as reflected by a substantial drop in Cy5 emission intensity for the conjugated compound compared to the fluorescence intensity of the Cy5 building block dye **1**. In the case of **RNP**, its Cy7 component exhibits very weak emission that is hardly enhanced when compared to free Cy7 building block dye **2** (Figure S4b), but the in the case of **RNP_{on}** the emission of its Cy7 component is greatly enhanced compared the corresponding free Cy7 building block dye **3** (Figure S4d). Importantly, the ratio of fluorescence intensities at the Cy5 and Cy7 maxima wavelengths (Cy7/Cy5 ratio) for **RNP_{on}** is significantly higher than for **RNP** (compare black spectral lines in Figure S4b and 4d). We infer from this data that **RNP** and **RNP_{on}** both exhibit energy transfer from the respective Cy5 donor to the Cy7 acceptor, but the Cy7 component in **RNP_{on}** has a 4'-carboxyl group and is more emissive.

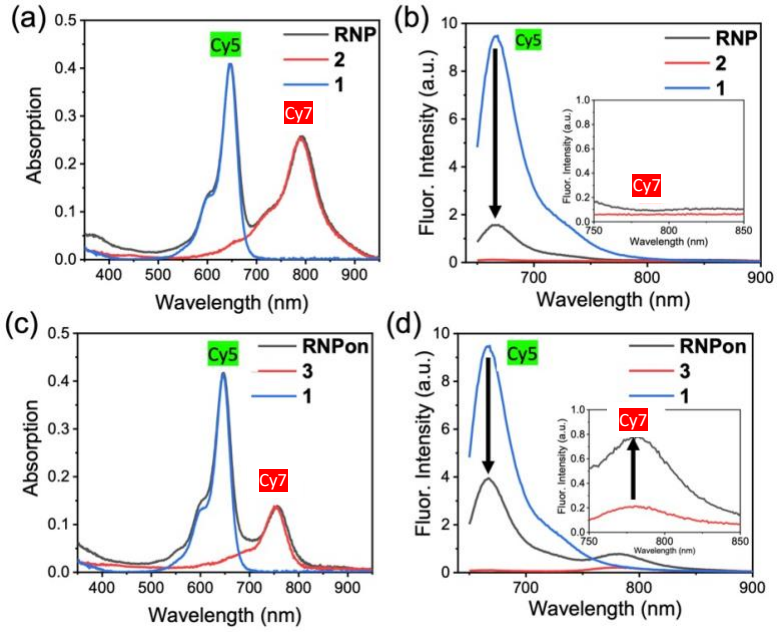

Figure S4. (a,c) Absorbance, and (b,d) Fluorescence spectra (λ_{ex} = 640 nm) of separate dye solutions in MeOH (4 μM) at room temperature. Slit width = 2 nm. The Cy5 and Cy7 peaks are indicated by colored labels.

6. Nitroreductase (NTR) Cleavage of RNP to Produce RNP_{on}

6.1 NTR cuvette studies

A 1 mM stock solution of **RNP** was prepared in DMSO. A 1 mg/mL stock solution of nitroreductase (NTR from *Escherichia coli*, purchased from Sigma Aldrich) was prepared in cold ultrapure water and preserved at −20 °C. A 10 mM stock solution of NADH was also prepared in cold ultrapure water when needed and stored at −20 °C. An aliquot of **RNP** (5 µM) was added to a cuvette containing 1× PBS Buffer, followed by the addition of NADH (500 µM) and NTR (10 µg mL^{-1}). The final mixture had a total volume of 1 mL and solutions were mixed by inversion for 5 seconds before monitoring changes in absorbance and fluorescence.

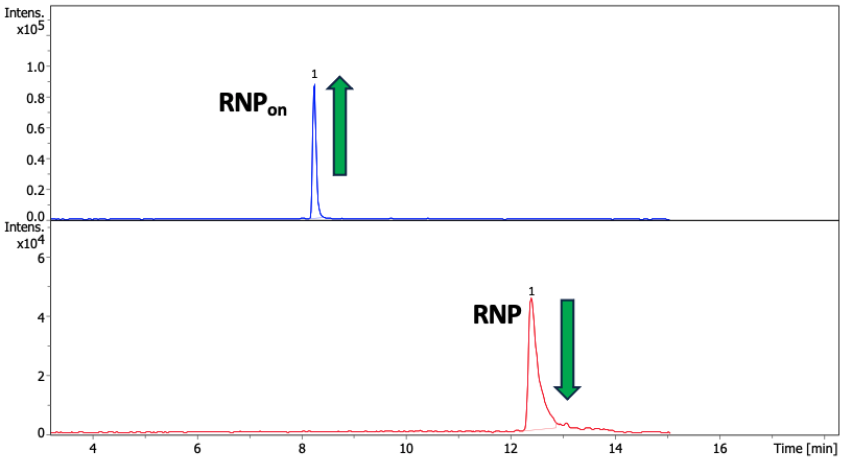

Figure S5. LC-MS (linear gradient 0-75% acetonitrile in water with 1 mM ammonium bicarbonate) showed that **RNP** was cleaved to produce $\mathbf{RNP_{on}}$. The peak at 12.5 min corresponds to **RNP** and the peak at 8.1 min corresponds to $\mathbf{RNP_{on}}$. The assignments were confirmed by injecting authentic samples.

7. RNP Binding by Bovine Serum Albumin (BSA)

Standard titration experiments added **RNP** to a solution of BSA and monitored quenching of the protein's tryptophan fluorescence.[5] A 1 mM stock solution of **RNP** was prepared in DMSO and a 2 µM stock of BSA was prepared in water. Aliquots of dye **RNP** (4 µL) were added to the BSA followed by a 5-minute incubation at 37 °C. The BSA tryptophan fluorescence intensity (ex: 280 nm, slit width: 2 nm) was plotted as a function of dye concentration and the relative fluorescence intensity at 345 nm was determined using the following equation, Relative fluorescence intensity = $(F_o - F)/F$ where F_o is the initial fluorescence intensity, F is the fluorescence intensity after each added aliquot of dye. The slope of the trend line (m) corresponds to 62,000 M^{-1} (Figure S6a) which is more than an order of magnitude weaker than BSA binding of more lipophilic heptamethine cyanine dyes such as indocyanine green (ICG). A near-infrared fluorescence experiment demonstrated that binding of **RNP** by BSA was not strong enough to inhibit NTR-mediated conversion of **RNP** to $\mathbf{RNP_{on}}$ (Figure S6b). Moreover, a fluorescence spectrum **RNP** in 100% Human Serum (HS) after one hour incubation at 37 ºC showed no measurable conversion to $\mathbf{RNP_{on}}$ (Figure S6c). Together, these results support the feasibility of **RNP** as an NTR-responsive probe for eventual use in living humans or human samples.

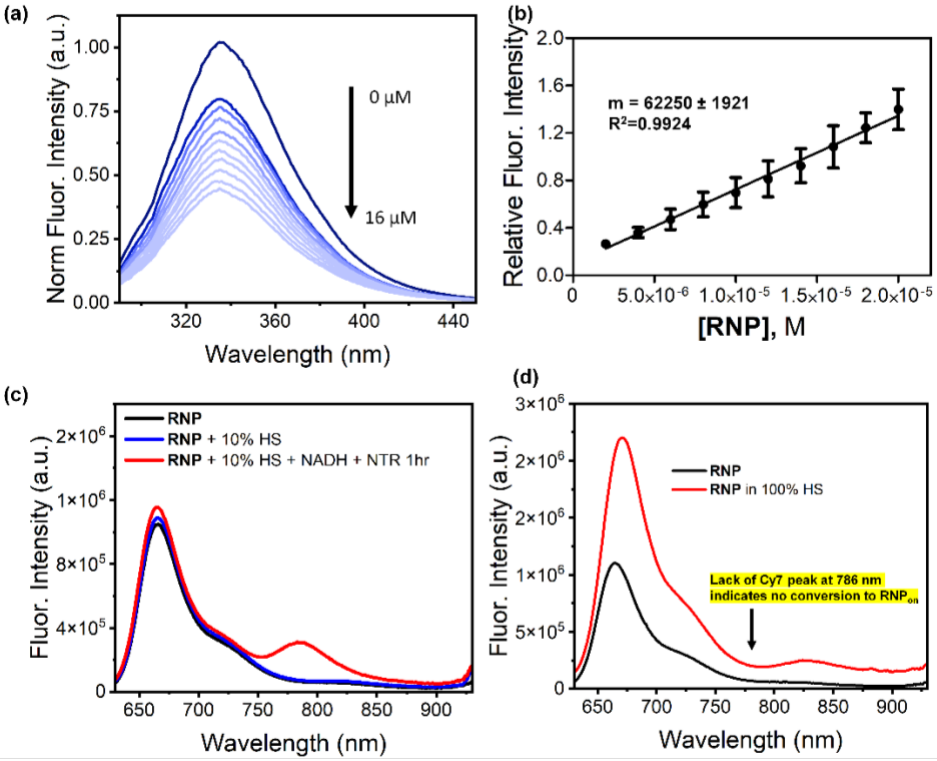

Figure S6. (a) Change in normalized fluorescence spectra of BSA tryptophan emission (ex: 280 nm) upon titration with **RNP** at 37 °C. (b) Graph provides association constant (m) = 62,000 ±1921 M^{-1} for binding of **RNP** by BSA. The albumin binding studies were repeated 3 times. (c) Fluorescence spectra showing that the presence of 10% human serum (HS) does not stop the NTR conversion of **RNP** into **RNP$_{on}$** at 37 ºC (samples contained 5 µM **RNP**, 500 µM NADH, 10 µg/ml NTR in 1X PBS buffer, ex: 620 nm, slit width = 5 nm (d) Fluorescence spectra showing that **RNP** in 100% human serum (HS) is not converted to **RNP$_{on}$** after one hour at 37 ºC, ex: 620 nm; slit width = 5 nm. The same high stability was observed in culture media.

7.1 Summary of probe photostability

The photostabilities of the two probes **RNP** and **RNP$_{on}$** mirrored the known photostabilities of the individual building blocks. That is, the common Cy5 component within each structure was not changed by long exposure to laboratory light or the low photon density used for all spectroscopy and imaging techniques. Cy7 dyes are known to be more photosensitive but there was a noticeable photostability difference between the two Cy7 components in **RNP** and **RNP$_{on}$** due to the difference in structures. The Cy7 component in **RNP** is partially quenched due to the appended 4'-nitrobenzyl ester group and as a result it is not changed by long exposure to laboratory light and the low photon density used for all spectroscopy and imaging techniques. Thus, **RNP** probe is quite stable to long term storage and moderate light exposure which is highly desired. The Cy7 component in **RNP$_{on}$** is more emissive due to the appended 4'-carboxyl group and this generated some reactive oxygen species that in turn produced minor photo-instability. This was not a technical problem because it was easy to protect **RNP$_{on}$** from the extraneous light during the short periods required to measure its appearance due to NTR activity.

7.2 NTR Michaelis Menten kinetics

To measure the Michaelis Menten Kinetics, different concentrations of **RNP** (0.5, 1, 2, 5, 7, 10, 15 µM) were incubated with NADH (500 µM) and NTR (1 µg mL^{-1}). Each reaction was monitored for a total of 5 minutes with 30 second interval readings. The initial rate of each reaction was then calculated using origin and a Lineweaver Burk plot along with a Michaelis Menten plot was generated and the K_m and V_{max} values were calculated using origin and Graph pad prism.

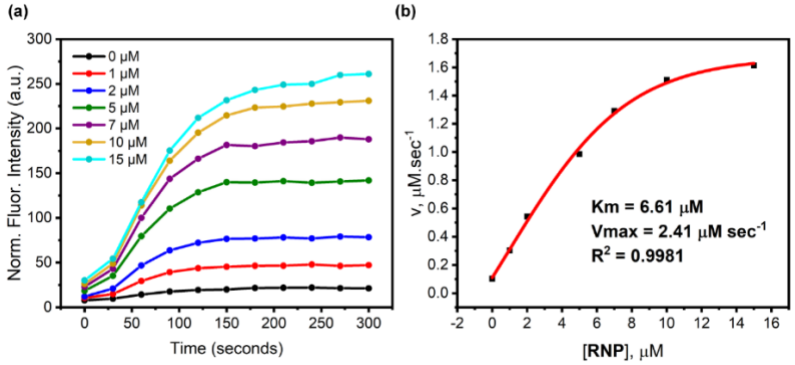

Figure S7. (a) Normalized fluorescence intensity-time graph of different concentrations of **RNP** (0-15 µM) + 500 µM NADH + 10 µg/mL NTR after 300 seconds. Data was collected at 20 second intervals at 37 ºC. (b) Michaelis Menten plot showing calculated K_m and V_{max} values of **RNP**. Slit width: 5 nm.

7.3 NTR limit of detection

A total of 5 µM **RNP** was incubated with 500 µM NADH and different concentrations of the NTR enzyme (1-10 µg/mL). The limit of detection (LOD) was obtained according to the equation LOD = 3σ/k, where σ is the standard deviation of ten measurements of blank sample (no NTR was added), and k is the slope of the linear relationship between fluorescence intensity of the probe and NTR concentration.

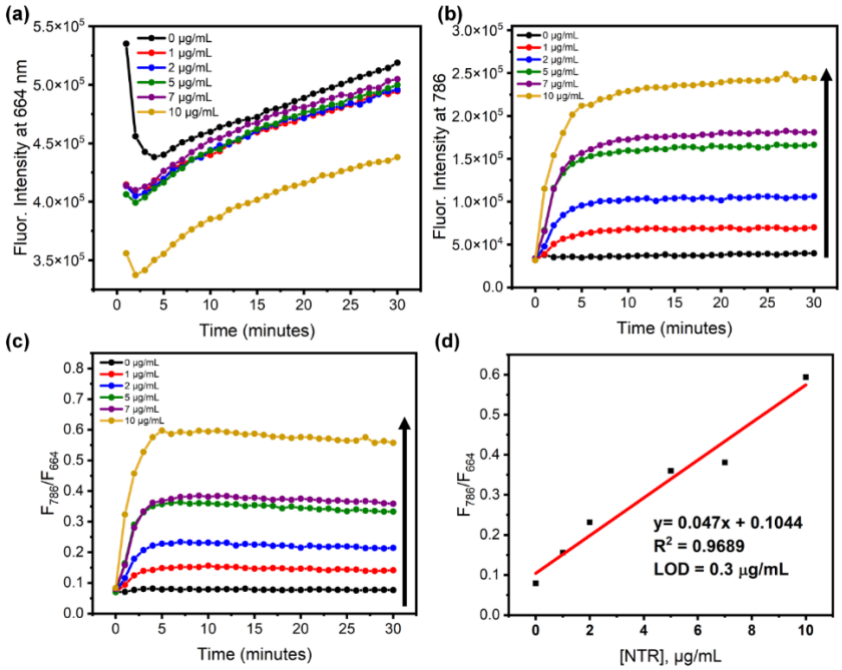

Figure S8. Fluorescence-time graph at wavelengths (a) 664 nm, (b) 786 nm and (c) 786/ 664 nm of 5 µM **RNP** + 500 µM NADH + different concentrations of NTR (0-10 µg/mL) in 1X PBS Buffer, ex: 620 nm, slit width = 5 nm at 37 ºC. (d) The calculated LOD value NTR using **RNP** as the substrate. The Limit of Detection (LOD) was calculated using the formula above.

7.4 NTR inhibition studies

A 10 mM stock solution of dicoumarol was prepared in DMSO and stored at room temperature. An aliquot of **RNP** (5 μM) was added to a cuvette containing 1× PBS Buffer, followed by the addition of 200 μM dicoumarol and NADH (500 μM) and NTR (1 μg mL^{-1}). The final mixture had a total volume of 1 mL and solutions were mixed by inversion for 5 seconds before monitoring changes in absorbance and fluorescence.

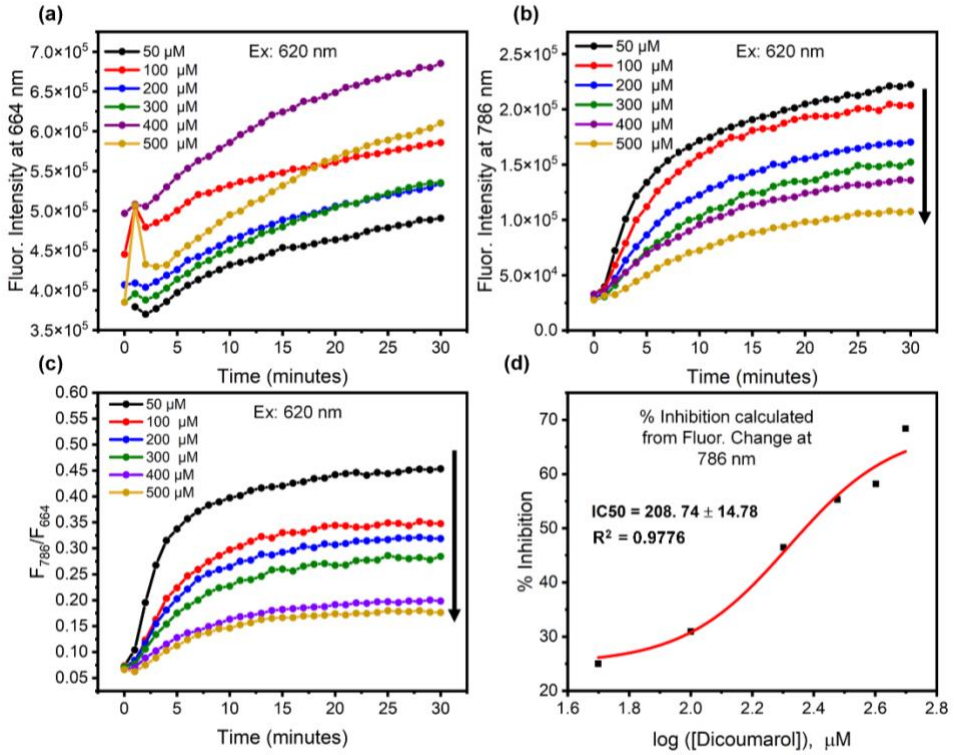

Figure S9. Dicoumarol inhibition of NTR enzyme. Fluorescence-time graph at wavelengths (a) 664 nm, (b) 786 nm and (c) 786/ 664 nm of 5 μM **RNP** + 500 μM NADH + different concentrations of Dicoumarol (50-500 μM) + 10 μg/ml NTR in 1X PBS Buffer, ex: 620 nm, slit width = 5 nm at 37 ºC. (d) The IC_{50} value for dicoumarol inhibition of NTR enzyme was determined to be 208 μM.

7.5 Imaging NTR activity using an In Vivo Imaging Station (IVIS)

A commercial IVIS (AMI HT Imaging) with Cy5 and Cy7 filter sets was used to acquire fluorescence images of a 96 well plate containing different concentrations of **RNP** (0-10 μM) and different [NTR] (0-10 μg/mL and 500 μM NADH after a 30-minute incubation at room temperature. Acquisition parameters: exposure time: 3 seconds, percent power: 50%, F-Stop: 2, FOV: 20, binning: Low, Cy5: excitation: 605/20 nm, emission: 670/20 nm, Cy7: excitation: 745/20 nm, emission: 850/20 nm. Images were analysed using image J software. Each ratiometric image was produced by first performing a background subtraction using a rolling ball 50-pixel radius, then the image was generated using the Image Calculator method. The mean pixel intensities of the Cy5 and Cy7 images were directly measured using a circle to generate a region of interest (ROI).

8. Two-Dimensional Cell Culture Studies

8.1 Cell culture

A549 human lung adenocarcinoma (ATCC® CCL-185™), HT-29 human colorectal adenocarcinoma (ATCC HTB-38), MDA-MB-231 human breast adenocarcinoma (ATCC HTB-26), U87 human glioblastoma (ATCC® HTB-14™), and CHOK1 chinese hamster ovarian cells were cultured in F12K Media, McCoy's 5A media, DMEM media and F12K media supplemented with 10% fetal bovine serum, 1% penicillin streptomycin respectively. Culture temperature was 37 °C using air supplemented with 5% CO_2.

8.2 Cell metabolic activity measurements

Standard MTT assays were used to measure cellular metabolic activity as an indicator of cell viability and probe cytotoxicity. A549, HT-29, MDA-MB-231 and CHOK1 cells were seeded in 96 well plates at a density of 5×10^3 cells per well and grown to 80% confluency for 48 hours at 5% CO_2 atmosphere. The media was removed, and plates were incubated under normoxic (20% O_2) or hypoxic (1% O_2) conditions for 24 hours (still containing 5% CO_2) at 37 °C. Different concentrations of **RNP** were then added to cells for 24 hours. The media containing **RNP** was removed and fresh medium containing 3-(4,5-dimethylthiazol-2-yl)-2,5-diphenyltetrazolium bromide (MTT) was added to cells for an additional 4-hour incubation (hypoxia: 1% O_2 and normoxia: 20% O_2). After 4 hours, SDS-HCl was added to wells to dissolve MTT crystals, and the cells were incubated overnight at 37 °C. The absorbance at 570 nm was then measured and a plot of the cell metabolic activity was obtained under each condition. All experiments were repeated three times to give an average activity, with error bars reflecting standard deviation.

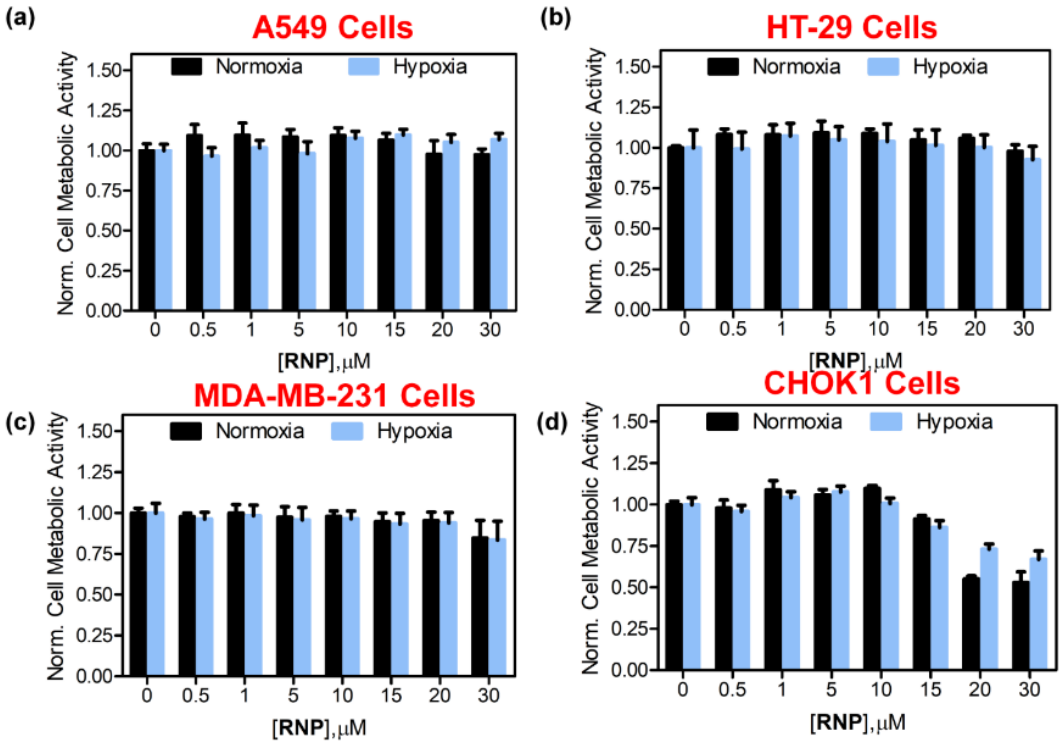

Figure S10. Cell Metabolic Activity of A549, HT-29 MDA-MB-231 and CHOK1 cells treated with **RNP** probe (0-30 μM) for 24 h under hypoxic or normoxic conditions.

8.3 Cell microscopy

A549 cells were plated onto 35 mm dishes and grown to 80% confluency (24 hours) under normoxic conditions. The media was removed, and the cells were washed with PBS twice. The media was replaced, and cells were grown at 37 °C for 24 hours in a Biospherix C Chamber housed inside the cell culture incubator. The incubator maintained hypoxic (1% O_2) or normoxic (20% O_2) atmosphere (also containing 5% CO_2) using functionalized gas controls and nitrogen gas to achieve low oxygen levels. After incubating cells under normoxic or hypoxic conditions, **RNP** (10 μM) was added, and the cells were further incubated under hypoxic or normoxic conditions for 1 hour. The media was removed, and the cells were washed three times with PBS. The cells were then fixed in cold 4% paraformaldehyde for 20 minutes at room temperature. The fixed cells were washed twice with PBS buffer and subsequently stained with Hoechst (3 μM) for 10 min and imaged using a Keyence BZ-X810 microscope using the following emission filter channels: DAPI (435-485nm), Cy5 (663-737 nm), Cy7 (780-900 nm). All microscopy experiments were repeated three times and micrographs of 6 separate viewing fields were obtained during each trial and analyzed using image J software. For each micrograph, a background subtraction with a rolling ball radius of 50 pixels was applied. A triangle threshold was employed to calculate the average Mean Pixel Intensity (MPI) along with SEM, and the values were plotted using GraphPad Prism. *p* values were calculated using *t* tests with ANOVA.

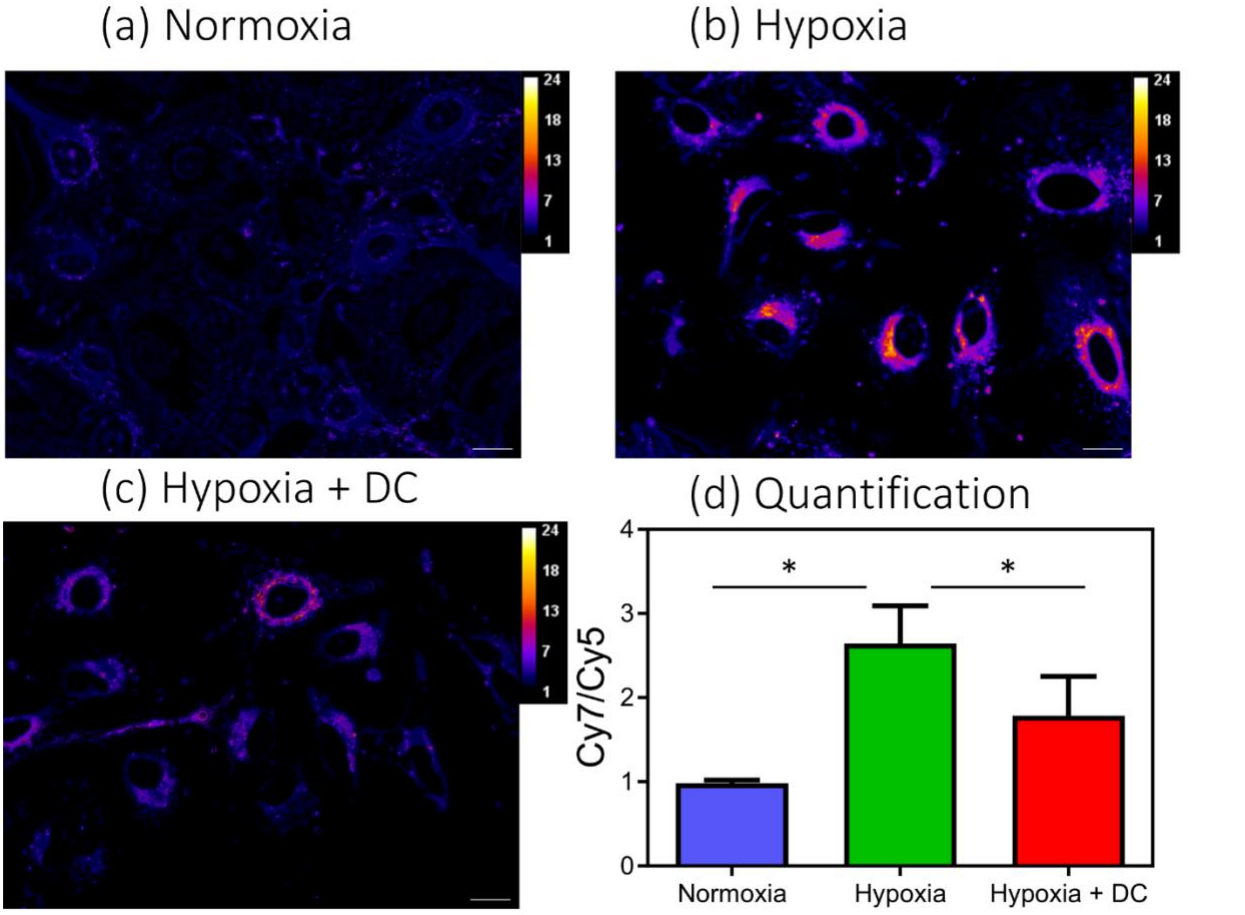

Figure S11. Representative ratiometric (Cy7/Cy5) fluorescence micrographs of (a) normoxic (20% O_2), or (b) hypoxic (1% O_2) A549 cells after incubation with 10 μM of **RNP** for 1 h. (c) Nitroreductase (NTR) inhibition was achieved by treating hypoxic cells with 200 μM dicoumarol (DC) before the addition of 20 μM **RNP** for 1 h. (scale bar = 40 μm) (d) Average Cy7/Cy5 ratio determined by measuring mean pixel intensity (MIP) for six separate micrographs per condition. Emission filter wavelengths: Cy5 (663-737 nm), Cy7 (780-900 nm). *p < 0.05.

9. Three Dimensional Tumor Spheroid Studies

9.1 Tumor spheroid formation and fluorescence imaging

Spheroids with a diameter range of 400-450 µm were formed using the hanging drop method.[7] Methylcellulose (6 g) was prepared in DMEM media (500 mL). The solution was stirred and spanned at 2500 g for 4 hours and subsequently stored at 4 ºC. To prepare spheroids, HT-29 and/or U87 cells were trypsinized and resuspended in McCoy's 5A media or DMEM media, respectively. Cells were centrifuged for 10 minutes at 0.2 rcf to form a pellet in a 15 mL tube. The media was then removed, and cells were resuspended in 1 mL of media and counted using trypan blue on a hemocytometer. A total of 400,000 HT-29 or U87 cells were then prepared in a total of 1 mL of McCoy's 5A or DMEM media containing 20% Methylcellulose to ensure each spheroid had a cell count of 10,000 cells. Spheroids were then plated on the cover of 35 mm dishes. To ensure spheroids remained hydrated, PBS buffer was added to the well of each plate. Spheroids were allowed to form for 48 hours at 37 ºC under normoxic conditions. Once spheroids formed, they were resuspended in media and incubated under hypoxic (1% O_2) or normoxic (20% O_2) conditions for 24 hrs. A 20 µM solution of **RNP** was added to the spheroids in media, and the treated spheroids were incubated for 1 hr under hypoxic (1% O_2) or normoxic (20% O_2) conditions. Experiments that included NTR inhibition were performed by incubating spheroids in media containing 200 µM dicoumarol (DC) for 1 hr, followed by addition of **RNP** (20 µM) for another 1 hr incubation under hypoxic (1% O_2) conditions. At the end of all experiments, the media was carefully removed, and the spheroids washed once with PBS buffer, then fixed in 4% paraformaldehyde at room temperature for 20 minutes. The paraformaldehyde was removed, and spheroids were washed once with PBS buffer. Fresh PBS buffer containing 3 µM Hoechst stain was then added to the fixed spheroids. The fixed spheroids were imaged on a Keyence BZ-X810 microscope using 10x magnification and the following emission filter channels: DAPI (435-485nm), Cy5 (663-737 nm), Cy7 (780-900nm). Image quantification was achieved by viewing and analyzing separate fields using image J software. For each micrograph, a background subtraction with a rolling ball radius of 50 pixels was applied. A triangle threshold was employed to calculate the average Mean Pixel Intensity (MPI) along with SEM, and the values were plotted using GraphPad Prism. *p* values were calculated using *t* tests with ANOVA. Spheroid radial intensity profiles were generated using the Radial Profile plugin in ImageJ. The spheroid area was selected on the Cy5 images, and the function was used to generate integrated intensity for values as a function of distance from the spheroid center. The intensity values and radial distances were normalized to the maximum value for each image to compare relative distribution.

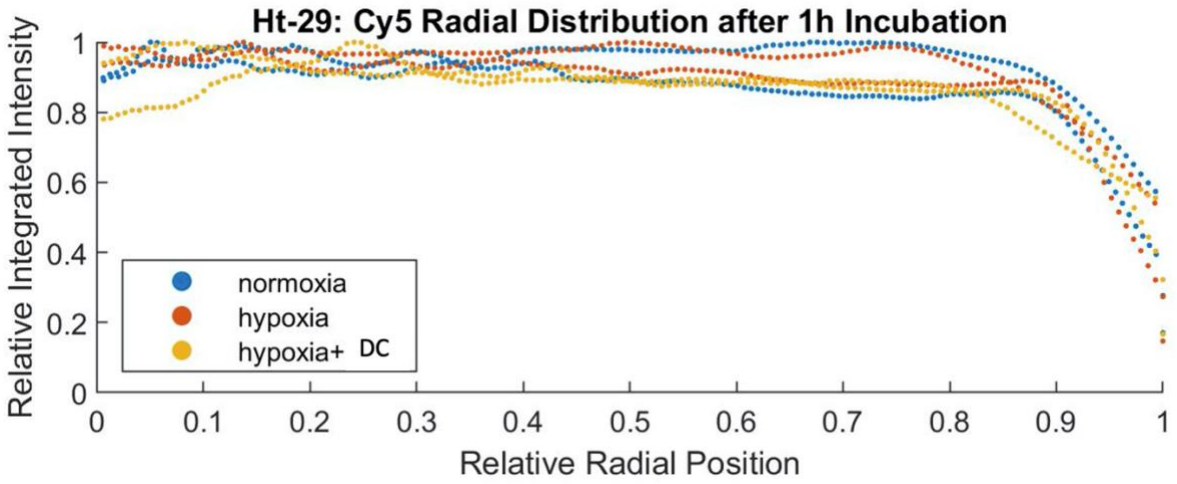

Figure S12: Radial distribution of normalized Cy5 emission intensity for **RNP** in HT-29 tumor spheroids described in manuscript Figure 4a. HT-29 cells grown under under normoxic (20% O_2) condition for 48 hours and then maintained under normoxic or hypoxic (1% O_2) condition for 24 hours (day 3) before being treated with **RNP** (20 µM) for 1 hour. NTR inhibition studies were performed by treating the hypoxic HT-29 spheroids with 200 µM dicoumarol (DC) for 1 hour before the addition of **RNP**. The spheroids were fixed in 4% paraformaldehyde and imaged with the emission filter channels, Cy5 (663-737nm), Cy7 (780-900nm). The plots indicate homogenous distribution of **RNP** throughout the spheroids.

(a)

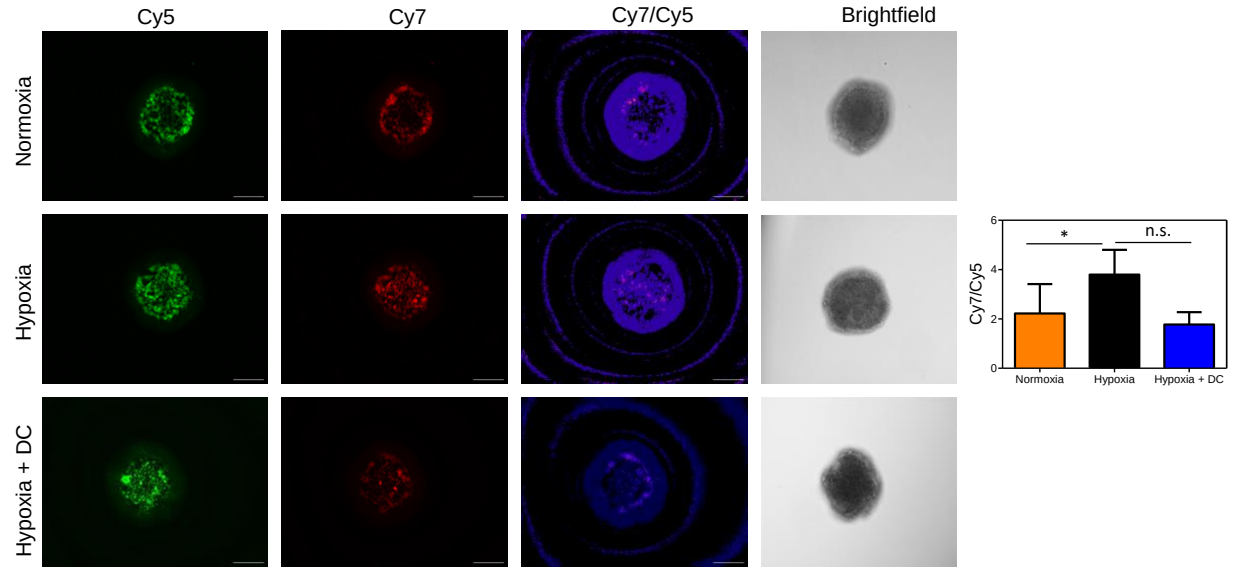

(b)

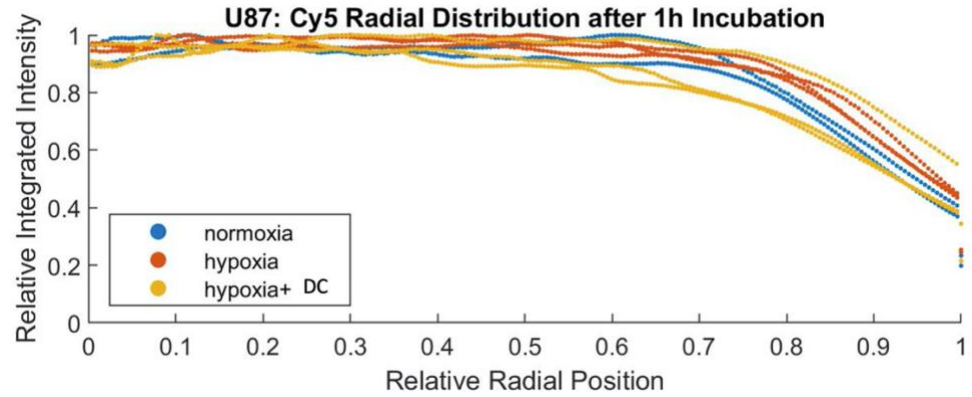

Figure S13: (a) Representative images of 3D tumor spheroids composed of U87 cells grown under normoxic (20% O_2) or hypoxic (1% O_2) conditions for 48 hours before being treated with **RNP** (20 μM) for 1 hour. NTR inhibition studies were performed by treating the hypoxic U87 spheroids with 200 μM dicoumarol (DC) for 1 hour before the addition of **RNP**. The spheroids were fixed in 4% paraformaldehyde and imaged with Keyence BZ-X810 microscope with emission filter channels, Cy5 (663-737 nm), Cy7 (780-900 nm). The bar graph shows quantification of average Mean Pixel Intensity (MPI) for N = 9 spheroids each for hypoxia and hypoxia condition where *$p \leq 0.05$, but N = 3 spheroids for hypoxia + DC condition, where the statistical assignment is n.s. (not significant) $p > 0.05$. Length scale 200 μm.
(b) Representative plots of radial distribution of normalized Cy5 emission intensity for **RNP** after 1 hour incubation with U87 tumor spheroids that had been maintained during day 3 under normoxic (20% O_2) or hypoxic (1% O_2) conditions. The plots indicate homogenous distribution of **RNP** throughout the spheroids.

9.2 Movies showing rotating z-stack images of fluorescent hypoxic cells within HT-29 tumor spheroids

The structured illumination feature of the Keyence BZ-X810 microscope was used to perform optical sectioning of the spheroids,[8] and two movie files are provided as Electronic Supplementary Information

<HT29 Spheroid Optical Section Normoxia RNP Cy7 Channel.mp4 >, 366 KB
<HT29 Spheroid Optical Section Hypoxia RNP Cy7 Channel.mp4>, 303 KB

The movies show rotating Z-stacks of Cy7-channel images (see Figure S14) representing central sections (100 µm thick) of the HT-29 spheroids grown under normoxic (20% O_2) or hypoxic (1% O_2) conditions and treated with **RNP**. Both movies show that the spheroid distribution of hypoxic cells, with enhanced Cy7 emission, is roughly even and apparently random with no evidence of a hypoxic spheroid core.

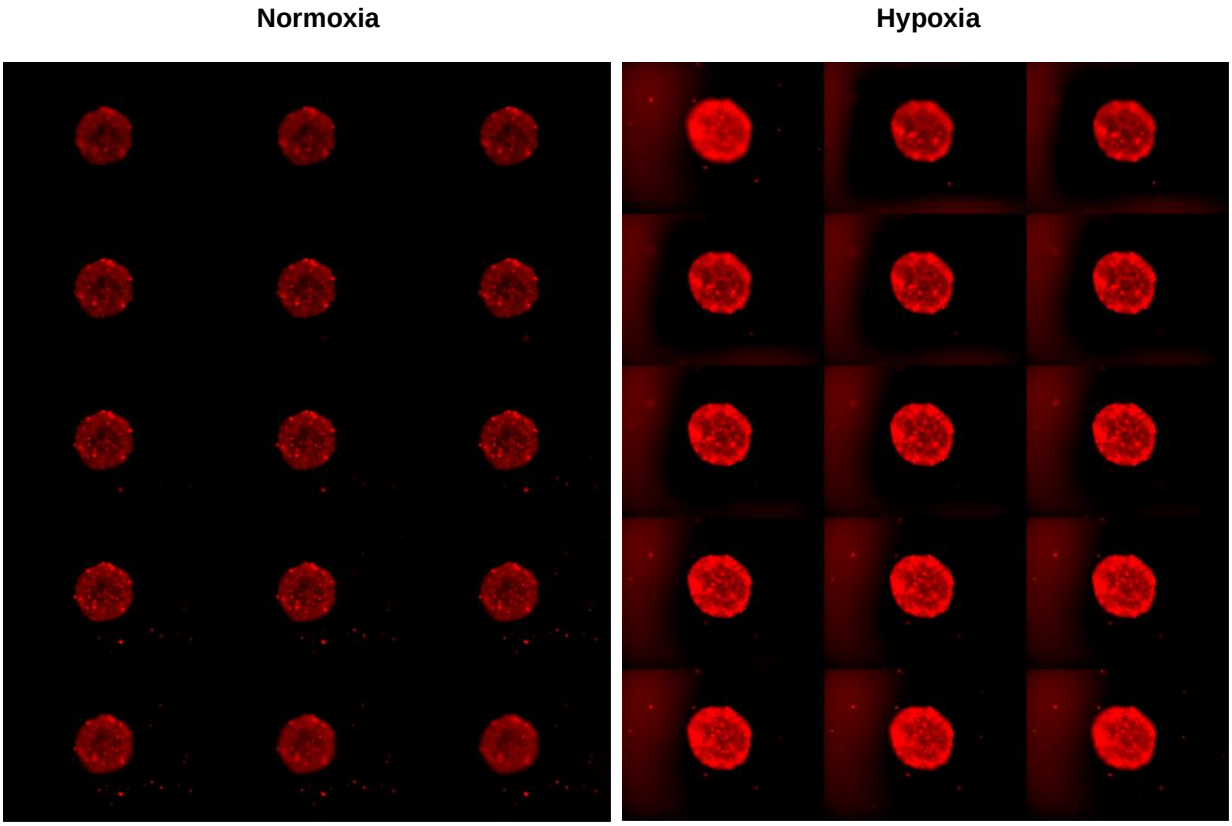

Figure S14: Optical sectioning movie montages showing every tenth Cy7-channel image within the central sections (100 µm thick) of intact HT-29 spheroids.

9.3 Immunohistochemistry analysis of spheroids

Spheroids were allowed to form for 48 hours at 37 ºC, then they were resuspended in media and incubated under hypoxic (1% O_2) or normoxic (20% O_2) conditions for 24 hrs. Spheroids were then fixed for 20 minutes in 4% paraformaldehyde and stored in 70% ethanol. To prepare spheroids for embedding in paraffin, the ethanol was exchanged with PBS1X after centrifuging (Minispin, Eppendorf) the spheroids by 5000 rpm for 3 min, and resuspending the cells 2 times with PBS 1 X respectively. Once the spheroids were suspended in PBS, 300 mL of agarose 2% (Agarose low melt, IBI Scientific) was added to the tube, gently hand agitated, and then centrifuged at 5000 rpm for 3 minutes to precipitate the spheroids in the tip of the microtube. Samples were kept at room temperature to ensure gel solidification. The agarose embedded spheroids were carefully removed from the microtubes by breaking a cotton swab and carefully using the pointed end of the swab applicator stick to remove the spheroids in gel from the tube. The entire sample was placed in an appropriately sized tissue cassette and placed in the tissue processor (Leica, TP 1020) overnight to infiltrate by paraffin. Paraffin infiltrated tissues were then embedded in a mold with liquid paraffin to form a block for better handling during microtome sectioning using a paraffin embedding station (Leica, Histo Core, Arcadia C). Sections with 6 µm thickness were obtained using a microtome (Leica, Histo core, Autocut R). For IHC staining, the slides were placed in a tissue staining dish and deparaffinization and rehydration were performed in a fume hood using the following sequence: Xylene 2x 5 min, 100% EtOH 5 min, 95% EtOH 5 min, 70% EtOH 5 min, Distilled H_2O 2 min. 1X citrate buffer was used for antigen retrieval via the Microwave method (WestingHouse, WCM110) heated twice, each time for 5 minutes at 50-H power. Blocking for endogenous peroxidase was done with 3% H_2O_2 for 5 minutes. After rinsing of the slides in TBST buffer, a pap pen (Liquid Blocker, Super Pap pen) was used for circling the tissue reducing the amount of reagent required for the following steps. The slides were placed in a humidified chamber and enough normal horse serum was applied to cover the tissue, (1-3 drops) from Vector ABC Universal RTU kit for 30 min. After draining excess blocking solution, the primary Ab was applied to the spheroid sections. The primary Abs against Ki67 (Rabbit mAb, abcam, Cat. No, ab 16667), caspase 3 (Rabbit pAb to caspase3, abcam, Cat. No. ab 4051), HIF-1alpha (Cell Signaling Technology, Cat. No. 3716S), Carbonic Anhydrase IX (pAb, Invitrogen, Lot. No. XD3548137) were diluted in TBST buffer in 1/100 ratio, applied to slides and incubated overnight to ensure that a proper binding reaction occurred. Secondary and tertiary antibody staining solutions were applied with Vector ABC Universal RTU kit for 30 min at room temp. TBST was used for rinsing the slides. For Antibody detection, DAB (3,3'-diaminobenzidine) solution in substrate was applied for 4 min at room temperature. Slides were then counterstained in hematoxylin for 1 min. Finally, dehydration and xylene steps were completed before mounting medium (Cytoseal XYL, Thermo Scientific) was applied for the application of the coverslip. The slides were imaged on a Leica Dmi1 inverted microscope at 10x magnification. The images of section spheroids were analyzed using a standard semi-quantitative protocol.[9] In short, each image contained between one and four sectioned spheroids and Fuji software within the Image J package was used to analyze the images in .tiff format by deconvoluting the image colors into blue/purple (nuclei stained by hematoxylin) and brown (antibody induced polymeric DAB) and quantifying the ratio of pixel intensities as a measure of protein expression.

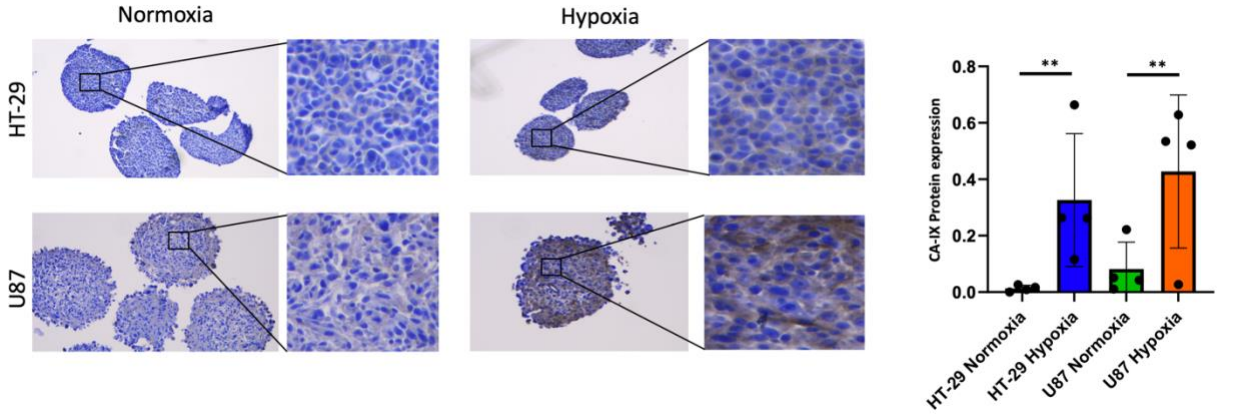

Figure S15: Representative immunohistochemistry staining of HT-29 and U87 spheroids for the presence of hypoxia biomarker, carbonic anhydrase IX (CA-IX). For each cell-line, a total of four images of sectioned spheroids were analyzed per condition, and scatter plots of the data reveal higher CA-IX protein expression (ratio of DAB staining per nuclei) for hypoxic spheroids compared to normoxic counterparts, indicating more CA-IX is expressed in the hypoxic spheroids. **p ≤ 0.01

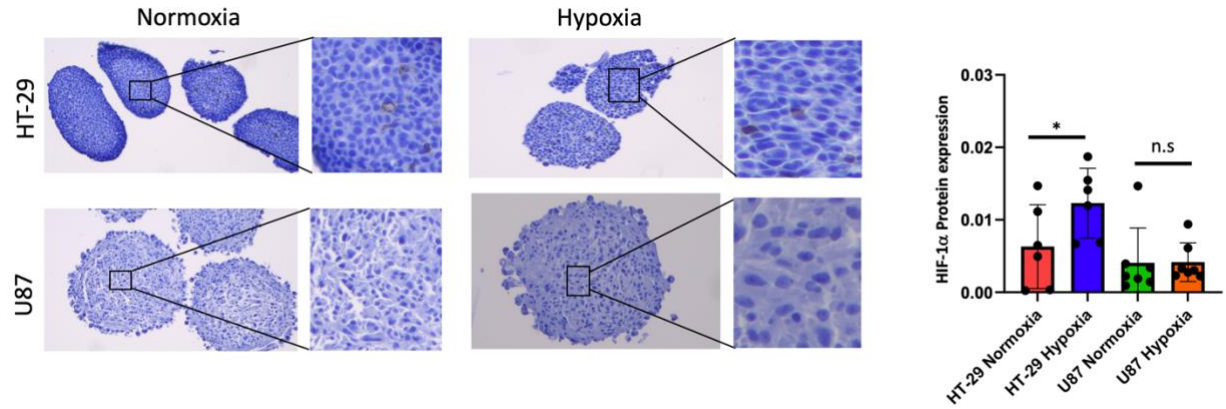

Figure S16: Representative immunohistochemistry staining of HT-29 and U87 spheroids for the hypoxia biomarker, hypoxia inducing factor 1α (HIF-1α). A total of six images of sectioned HT-29 spheroids were analyzed per condition, and scatter plots of the data reveal higher HIF-1α protein expression (ratio of DAB staining per nuclei) in hypoxic spheroids compared to their normoxic HT-29 spheroids, however, no statistical difference is seen between hypoxic and normoxic U87 spheroids (N = 7 images of spheroid sections per condition). n.s (not significant) p > 0.05, *p ≤ 0.05. The small number of black deposits in the images are DAB staining artifacts.

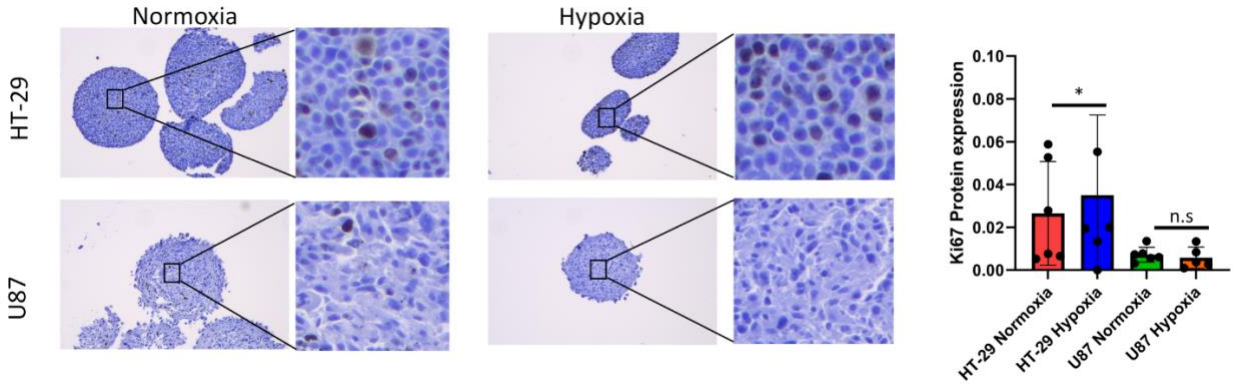

Figure S17: Representative immunohistochemistry staining of HT-29 and U87 spheroids for the proliferation biomarker, Ki67. A total of six images of sectioned spheroids were analyzed per cell-line and condition and all images showed that the spheroids had not developed a quiescent or necrotic core. Scatter plots of the data reveal higher Ki67 protein expression (ratio of DAB staining per nuclei) in hypoxic HT-29 spheroids compared to their normoxic HT-29 spheroids, however, no statistical difference is seen between hypoxic and normoxic U87 spheroids. n.s. (not significant) $p > 0.05$, $*p \leq 0.05$. The small number of black deposits in the images are DAB staining artifacts.

References:

[1] H. Hyun, M. Henary, T. Gao, L. Narayana, E. A. Owens, J. H. Lee, G. Park, H. Wada, Y. Ashitate, J. V. Frangioni and H. S. Choi, 700-nm zwitterionic near-infrared fluorophores for dual-channel image-guided surgery. *Mol. Imaging Biol*. **2016**, *18*, 52–61.

[2] K. M. Atkinson, J. J. Morsby, S. S. R. Kommidi and B. D. Smith, Generalizable synthesis of bioresponsive near-infrared fluorescent probes: sulfonated heptamethine cyanine prototype for imaging cell hypoxia. *Org. Biomol. Chem*. **2021**, *19*, 4100-4106.

[3] M. Gerowska, L. Hall, J. Richardson, M. Shelbourne and T. Brown, Efficient reverse click labeling of azide oligonucleotides with multiple alkynyl Cy-Dyes applied to the synthesis of HyBeacon probes for genetic analysis. *Tetrahedron* **2012**, *68*, 857-864.

[4] F. Rüttger, S. Mindt, C. Golz, M. Alcarazo and M. John, Isomerization and dimerization of Indocyanine Green and a related heptamethine dye. *European J. Org. Chem.* **2019**, *2019*, 4791–4796.

[5] M. Y. Berezin, K. Guo, W. Akers, J. Livingston, M. Solomon, H. Lee, K. Liang, A. Agee and S. Achilefu, Rational approach to select small peptide molecular probes labeled with fluorescent cyanine dyes for in vivo optical imaging. *Biochemistry* **2011**, *50*, 2691–2700.

[6] M. Ghasemi, T. Turnbull, S. Sebastian and I. Kempson, The MTT assay: utility, limitations, pitfalls, and interpretation in bulk and single-cell analysis. *Int. J. Mol. Sci.*, **2021**, *22*, 12827.

[7] M. J. Ware, K. Colbert, V. Keshishian, J. Ho, S. J. Corr, S. A. Curley and B. Godin, Generation of homogenous three-dimensional pancreatic cancer cell spheroids using an improved hanging drop technique. *Tissue Eng. - Part C Methods* **2016**, *22*, 312–321.

[8] J. D. Manton. Answering some questions about structured illumination microscopy, *Philos. Trans. R. Soc. A Math. Phys. Eng. Sci.* **2022**, *380*, 20210109.

[9] A. R. Crowe, and W. Yue, W, Semi-quantitative determination of protein expression using immunohistochemistry staining and analysis. *Bio-protocol* **2019**, *9*, 1–11.